



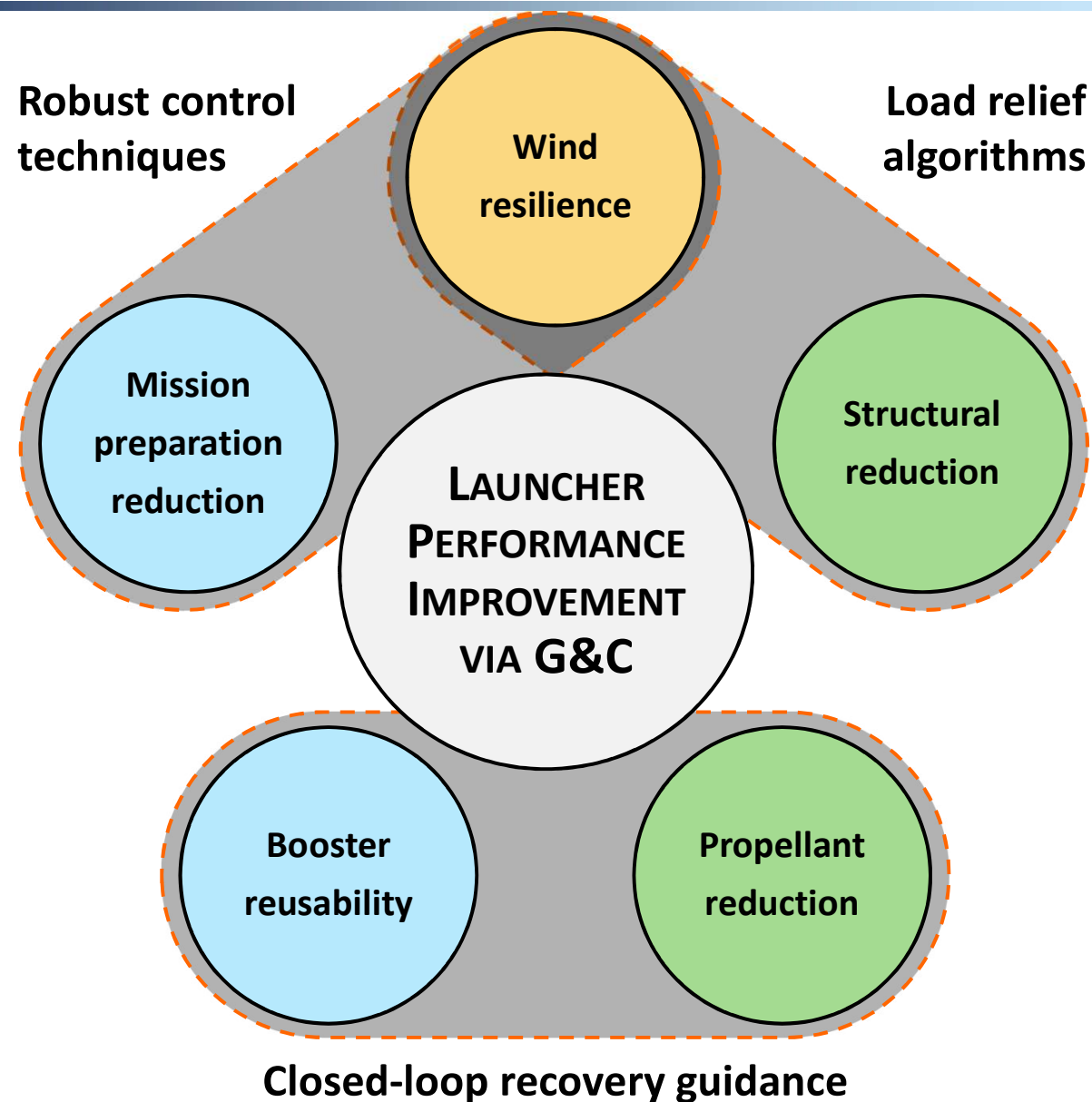
Advances in launcher guidance and control design: from robust control to convex optimization

Andrés Marcos
Diego Navarro-Tapia
Pedro Simplício

Technology for AeroSpace Control (TASC)
Aerospace Engineering Department
University of Bristol, U.K.
www.tasc-group.com

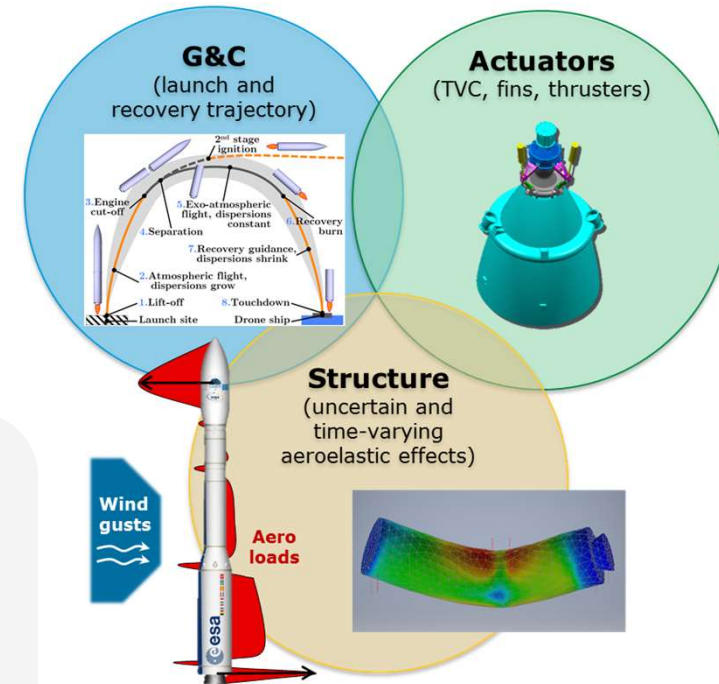
Samir Bennani

Guidance, Navigation and Control Section
European Space Agency, ESTEC



➤ Launcher G&C particularly **challenging** because:

- Mission/aerothermal requirements tend to **compete** against each other
- Strong **couplings** between trajectory, propulsion and flexible structure



Funded by an **ESA NPI contract** 4000114460/15/NL/MH/ats

“Robust & Adaptable Launcher TVC Control Systems for the VEGA Evolution”



Samir Bennani



Diego Navarro-Tapia
Andrés Marcos



Christophe Roux

Funded by an **ESA NPI contract** 4000119571/17/NL/MH

“Advanced Flight Control System Design With Active Load & Relief Capabilities”



Samir Bennani



Pedro Simplicio
Andrés Marcos



Stephan Theil
David Seelbinder

1. Ascent **Control**: robust → LPV → adaptive

- VEGA launcher case

2. Descent **Guidance**: convex pinpoint landing optimization

- VEGA-like reusable launch vehicle case

3. Ascent **Load Relief**: wind disturbance observer + fins

- VEGA-like reusable launch vehicle case

Ascent Control: robust → LPV → Adaptive

Funded by an **ESA NPI contract** 4000114460/15/NL/MH/ats

“Robust & Adaptable Launcher TVC Control Systems for the VEGA Evolution”



Samir Bennani



Diego Navarro-Tapia
Andrés Marcos



Christophe Roux

Diego Navarro-Tapia is also the recipient of a DTP award by the UK EPSRC



VEGA (Vettore Europeo di Generazione Avanzata)

is the new European Small Launch Vehicle



VEGA



Soyuz



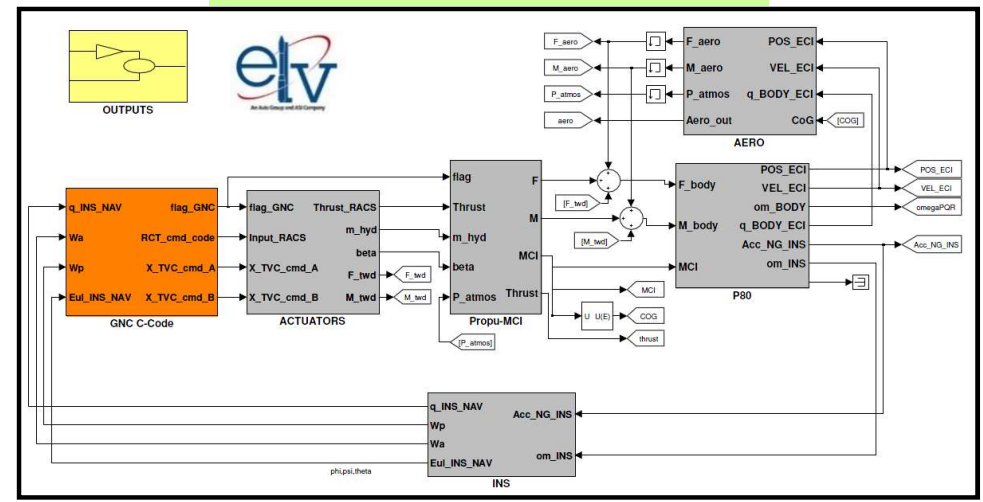
Ariane 5



Saturn V

13 successful flights ... 14th this month

VEGACONTROL
nonlinear, high-fidelity simulator for atmospheric phase



Over 120 uncertain parameters

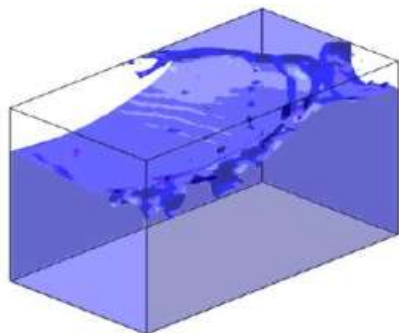
Type	Flag	Description
AEROELASTICITY	Flag aeroelastic	aero-elasticity effect (+10% on Cl coefficient)
	Flag disp_CA	Deperson on 1 st Stage Axial Coefficient
	Flag unc_CA	Uncertainty on 1 st Stage Axial Coefficient
AERODYNAMICS	Flag disp_CN	Deperson on 1 st Stage Normal Coefficient
	Flag unc_CN	Uncertainty on 1 st Stage Normal Coefficient
	Flag disp_Xcp	Deperson on 1 st Stage Xcp
	Flag unc_Xcp	Uncertainty on 1 st Stage Xcp
	Flag aero_roll	To enable Roll Motion
WIND	Flag azimuth_wind_angle	Wind azimuth direction (rad)
	Flag u_wind	Synthetic wind gust attitude (km)
IRS	Flag IRSmountingX	IRS Mounting Error um X Body Axis
	Flag IRSmountingZ	IRS Mounting Error um Z Body Axis
THRUST PARAMETER & SCATTERING	Flag dSP	1 st stage impulse scattering
	Flag dTC	Scattering on time burn
	Flag SRM_roll	Scattering on SRM Roll Torque
	Flag stagedM	Structural mass scattering
MCI	Flag stagedM_Prop	Scattering on propellant mass
	Flag stagedJx	Scattering on Stage XX MCI
	Flag stagedJy	Scattering on Stage YY MCI
	Flag stagedJz	Scattering on Stage ZZ MCI
	Flag stagedCOG	Scattering on X CoG
	Flag stagedCOG	Scattering on Y CoG
	Flag stagedX_B	Scattering on structural Stage XX MCI
	Flag stagedY_B	Scattering on structural Stage YY MCI
	Flag stagedZ_B	Scattering on structural Stage ZZ MCI
	Flag stagedCOG_B	Scattering on structural X CoG
Flag stagedCOG_B	Scattering on Y structural CoG	

Category	Flag	Description
MCI	Flag P1a0	Scattering on PL Mass
	Flag P1a1x	Scattering on PL XX MCI
	Flag P1a1y	Scattering on PL YY MCI
	Flag P1a1z	Scattering on PL ZZ MCI
	Flag P1a1COG	Scattering on PL X CoG
	Flag P1a1COG	Scattering on PL Y CoG
THRUST OFFSET & MISALIGNMENT	Flag P1a2a0	Scattering on TVC gain Lane 0
	Flag TVC_gain_L1a0	Scattering on TVC Lane 0 (Gaussian)
	Flag TVC_gain_L1a1	Scattering on TVC Lane 1 (uniform)
	Flag TVC_gain_L1a2	Scattering on TVC gain Lane 2
	Flag TVC_gain_L2a0	Scattering on TVC Lane 2 (Gaussian)
	Flag TVC_gain_L2a1	Scattering on TVC Lane 2 (uniform)
	Flag TVC_gain_L2a2	Scattering on thrust misalignment first lane (Gaussian)
	Flag TVC_gain_L2a3	Scattering on thrust misalignment second lane (Gaussian)
	Flag TVC_gain_L2a4	Scattering on thrust misalignment first lane (uniform)
	Flag TVC_gain_L2a5	Scattering on thrust misalignment second lane (uniform)
ATMOSPHERE SEPARATION DISTURB	Flag P1a2a1	Scattering on thrust offset in X
	Flag P1a2a2	Scattering on thrust offset in Y (Gaussian)
	Flag P1a2a3	Scattering on thrust offset in Z (Gaussian)
	Flag P1a2a4	Scattering on thrust offset in X (uniform)
	Flag P1a2a5	Scattering on thrust offset in Y (uniform)
	Flag P1a2a6	Scattering on thrust offset in Z (uniform)
	Flag P1a2a7	atmospheric Density

Four stages vehicle,
all controlled by **TVC**
thrust vectoring system



sloshing



Atmospheric phase challenges

Launch vehicle:

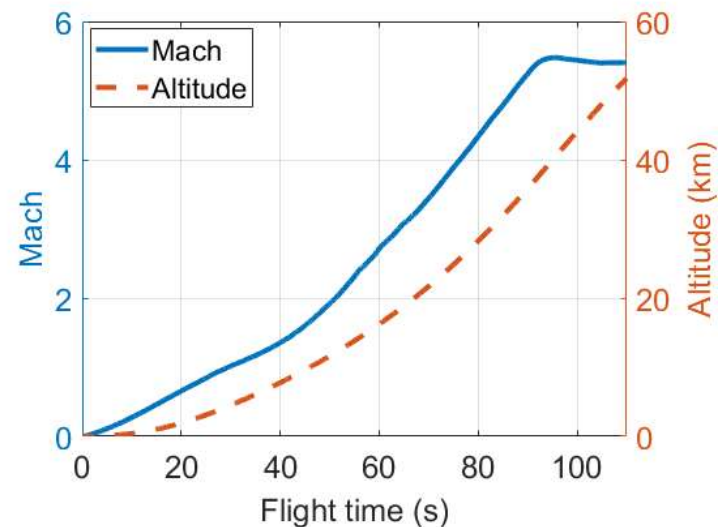
- Unstable
- Flexible structure
- sloshing

High variation of flight parameters

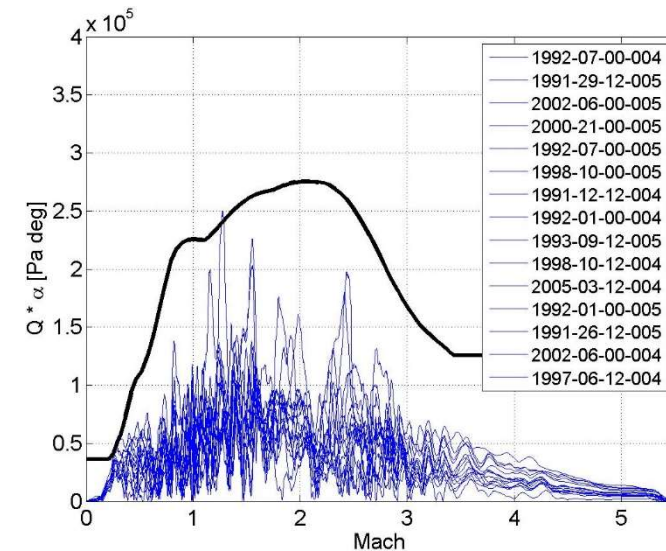
Challenging environment:

- Wind disturbances
- Structural loads (Q_{α})

VEGA VV05 mission

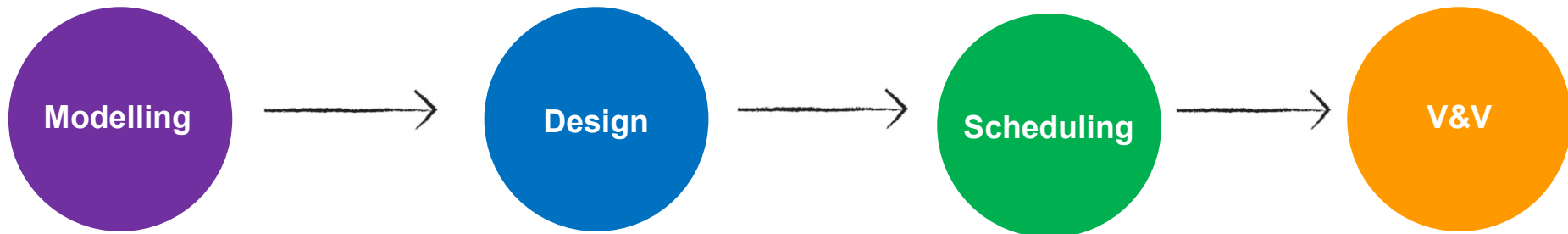


VEGA Q_{α} wind effect



Using **nominal** models

Using **perturbed** models



Launcher model linearised at representative points along trajectory

For VEGA ~every 10 sec

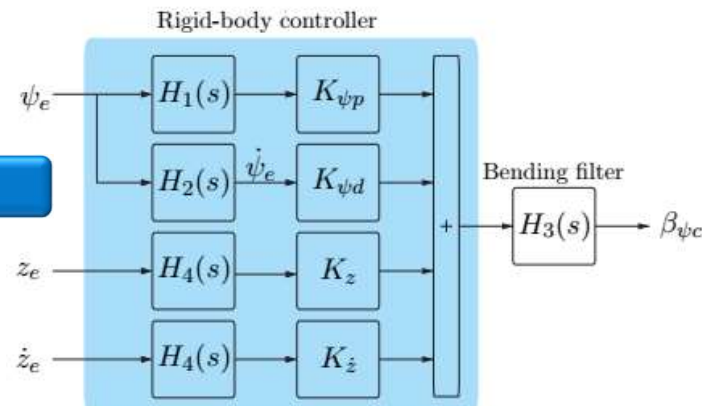
- 1 Rigid-body controller design
- 2 Bending filters design
- 3 Rigid- and flexible-body joint tuning

Ad-hoc scheduling based on some parameter (time, VNG)

Intensive V&V process using high-fidelity nonlinear simulator

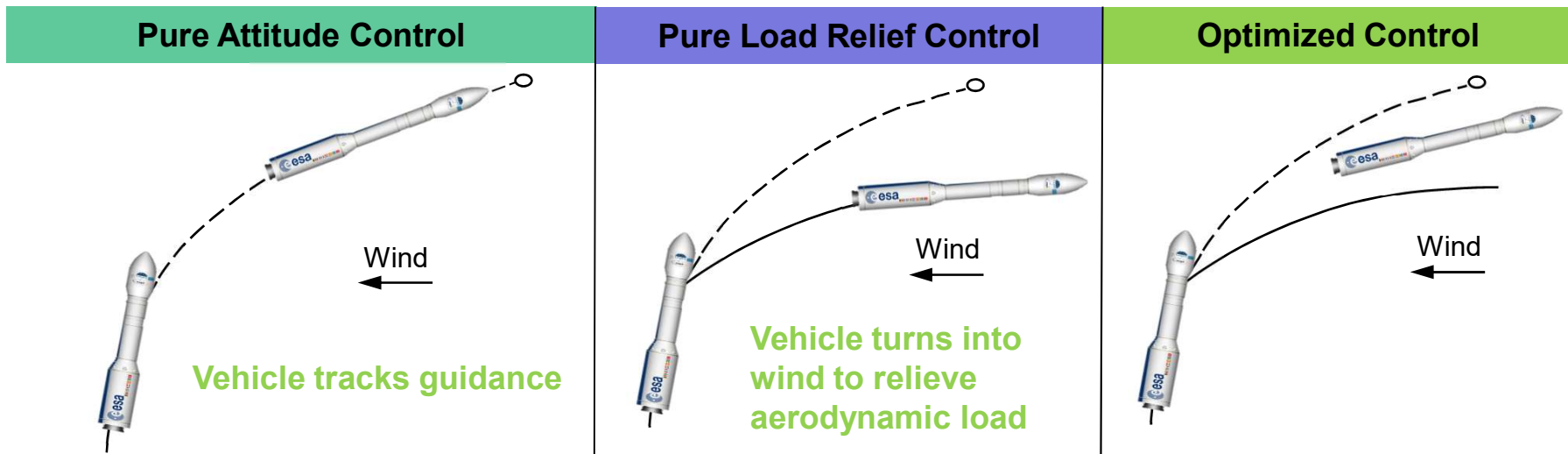
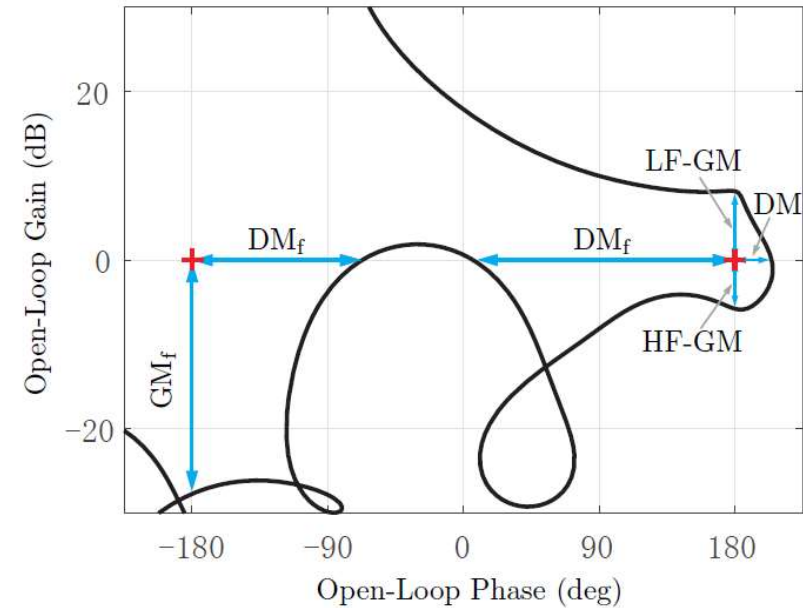
For VEGA
Monte Carlo &
Vertex simulations

VEGA TVC architecture



VEGA State-of-Practice: Control objectives & design rationale

	Requirements	Metrics	Bounds	
Stability	Rigid-body margins	LF-GM	Nominal	≥ 6 dB
			Dispersed	≥ 0.5 dB
		DM	Nominal	≥ 100 ms
			Dispersed	≥ 40 ms
		HF-GM	Nominal	≤ -6 dB
			Dispersed	≤ -3 dB
Flexible-body margins	GM _f	Nominal	≤ -3 dB	
		Dispersed	≤ -3 dB	
	DM _f	Nominal	≥ 50 ms	
		Dispersed	≥ 20 ms	



Ascent Control:

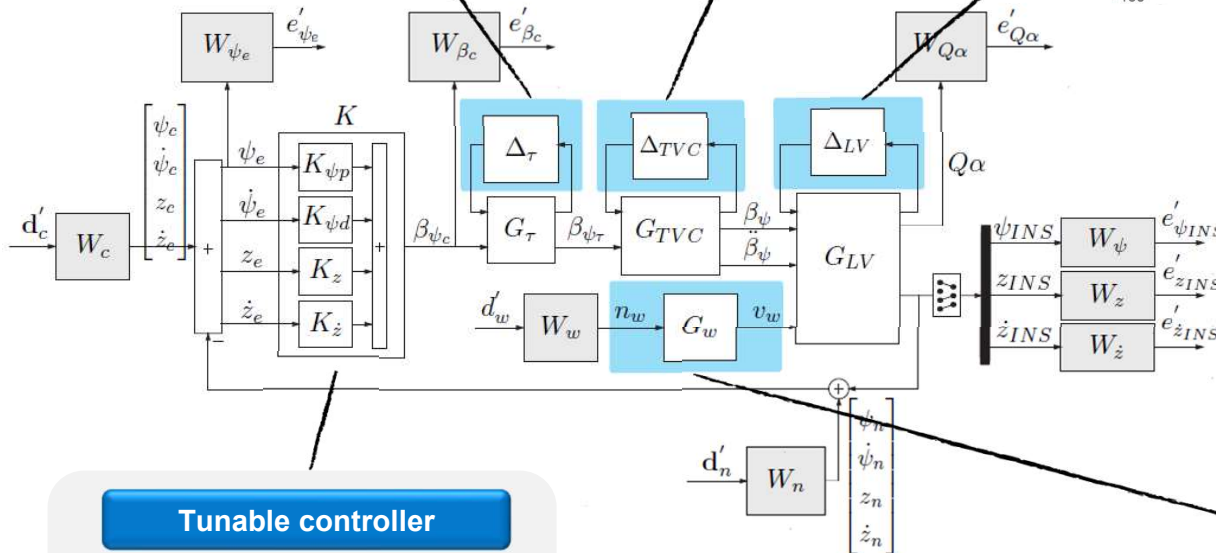
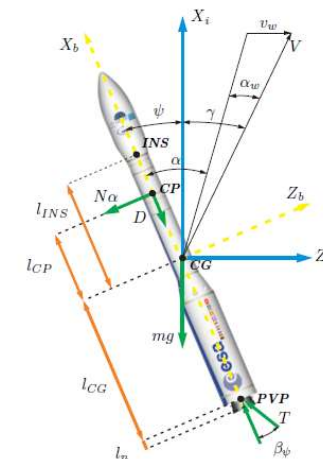
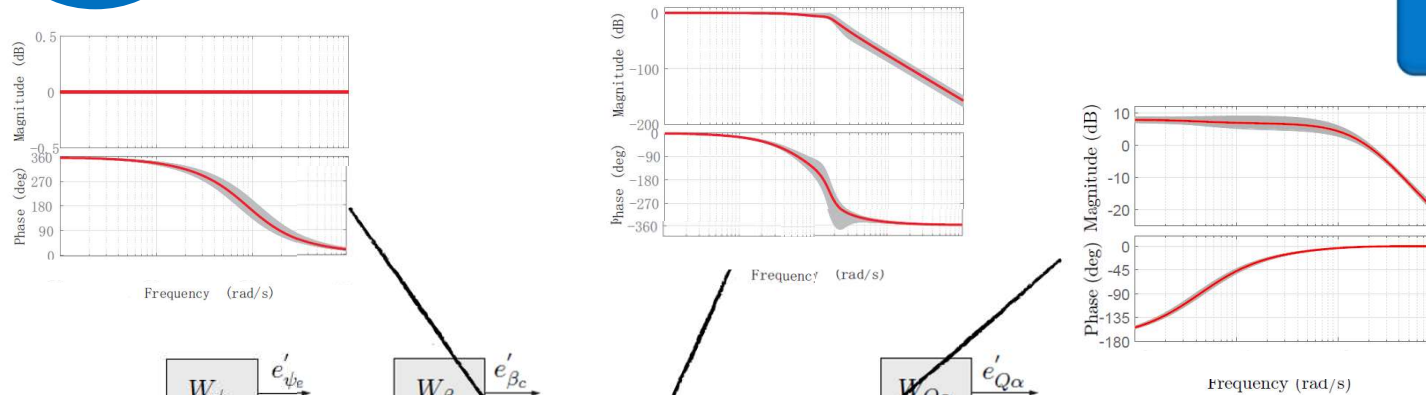
robust → LPV → Adaptive

VEGA Structured H_∞ synthesis: Rigid-body robust design



Rigid-body design can be **augmented** to account for statistical **wind levels** and **parametric uncertainties (LFT modelling)**

**Rigid-body
Launch vehicle model**



Tunable controller

- ❑ Rigid-body controller four parameters

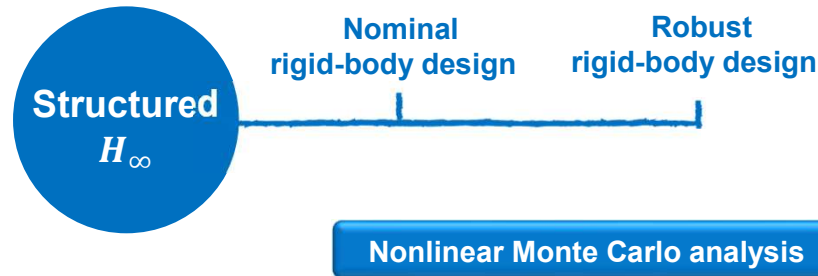
Wind generator

Wind model defined by a **Dryden filter** for severe turbulence:

$$G_w(s) = \frac{v_w(s)}{n_w(s)} = \frac{\sqrt{\frac{2}{\pi} \frac{V(h) - v_{wp}(h)}{L(h)} \sigma^2(h)}}{s + \frac{V(h) - v_{wp}(h)}{L(h)}}$$

VEGA Structured H_∞ synthesis:

Rigid-body robust nonlinear Monte Carlo analysis



In total, **9 linear structured H_∞ controllers** are synthesized along the atmospheric phase, and are scheduled using VNG (as in VEGA)

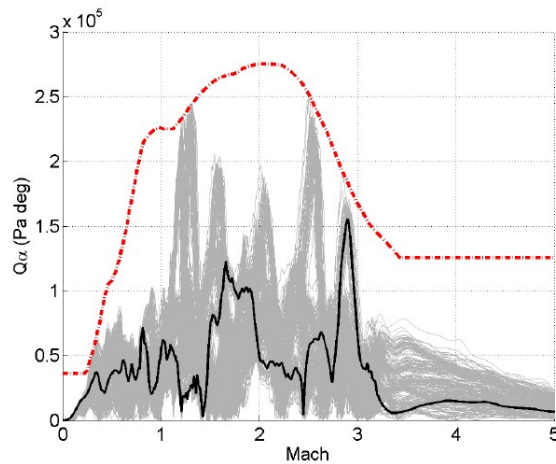
4 MC campaigns of 500 runs:
 Each MC used **same scattering flags**
 but a **different wind profile**

MC quantitative assessment

For each controller and each MC run, get the **∞ -norm** and **2-norm** for different performance indicators.

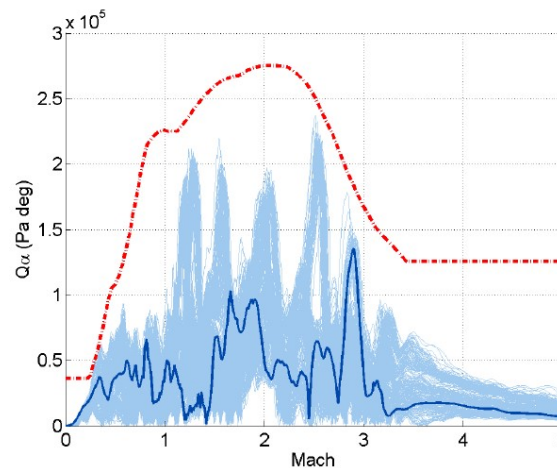
Results normalised wrt baseline controller

Baseline controller

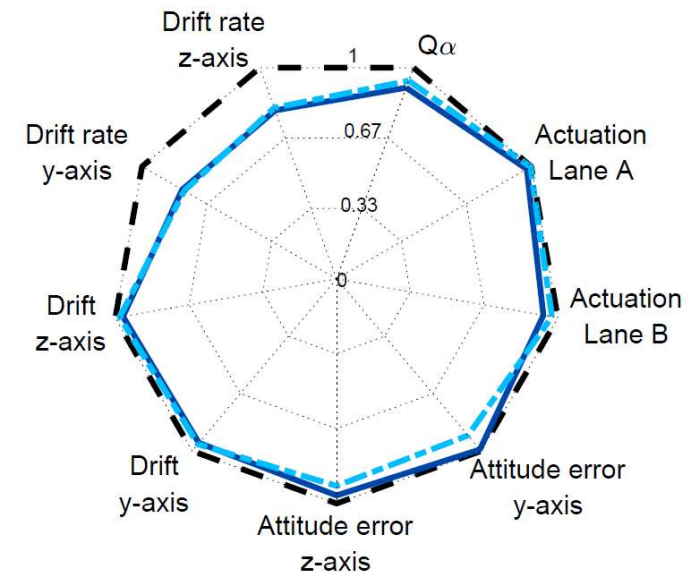


- - - Q_α envelope
— Baseline (nominal – wind VV05)
— Baseline (dispersed)

Rigid-Body Structured H_∞ controller

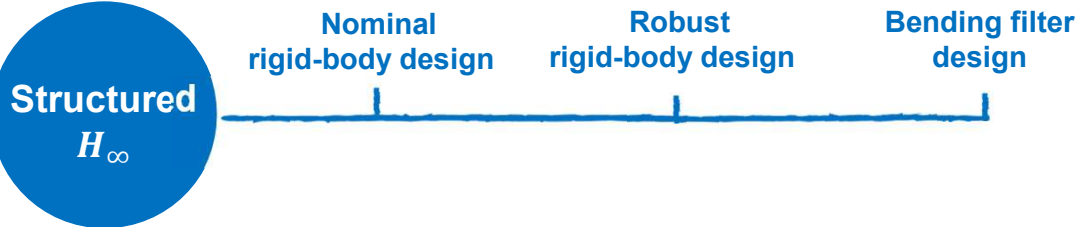


— Structured H_∞ (nominal – wind VV05)
— Structured H_∞ (dispersed)

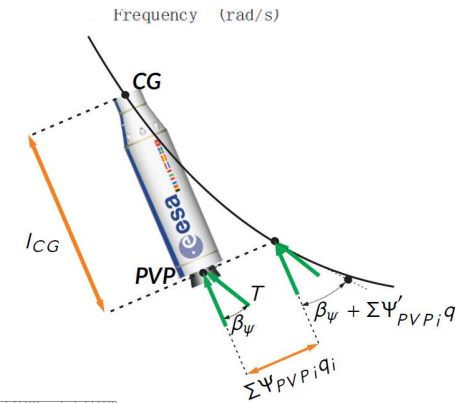
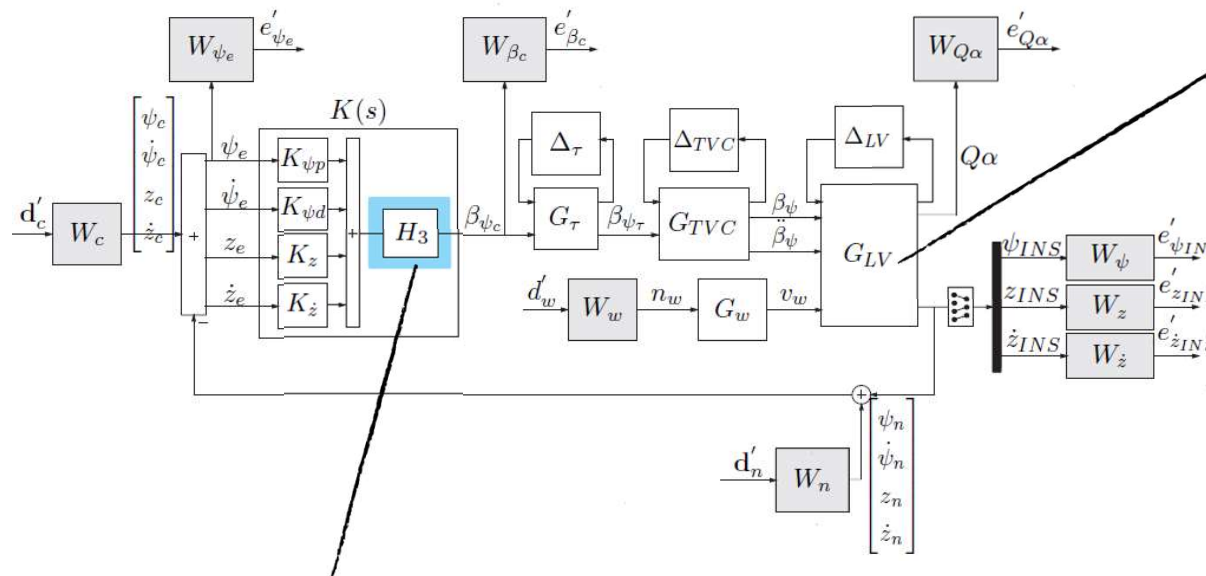
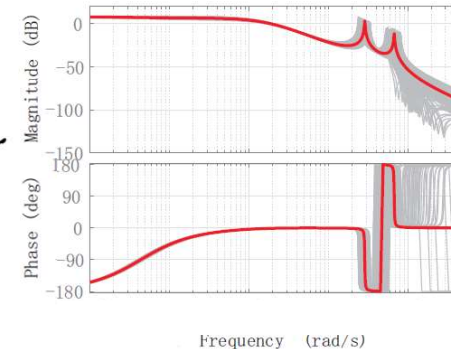


— Struc. H_∞ controller (∞ -norm)
- - - Struc. H_∞ controller (2-norm)

VEGA Structured H_∞ synthesis: Flexible sequential bending filter design



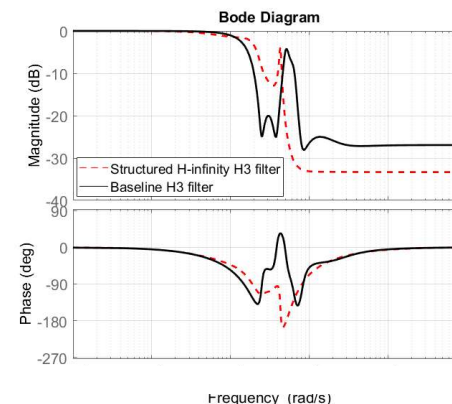
LFT launch vehicle model
Rigid-body and flexible dynamics



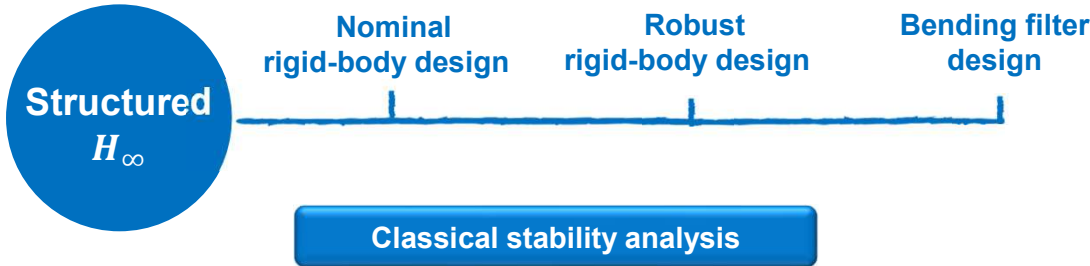
Tunable controller

- ❑ Rigid-body controller fixed as baseline controller
- ❑ Tunable bending filter (6 parameters)

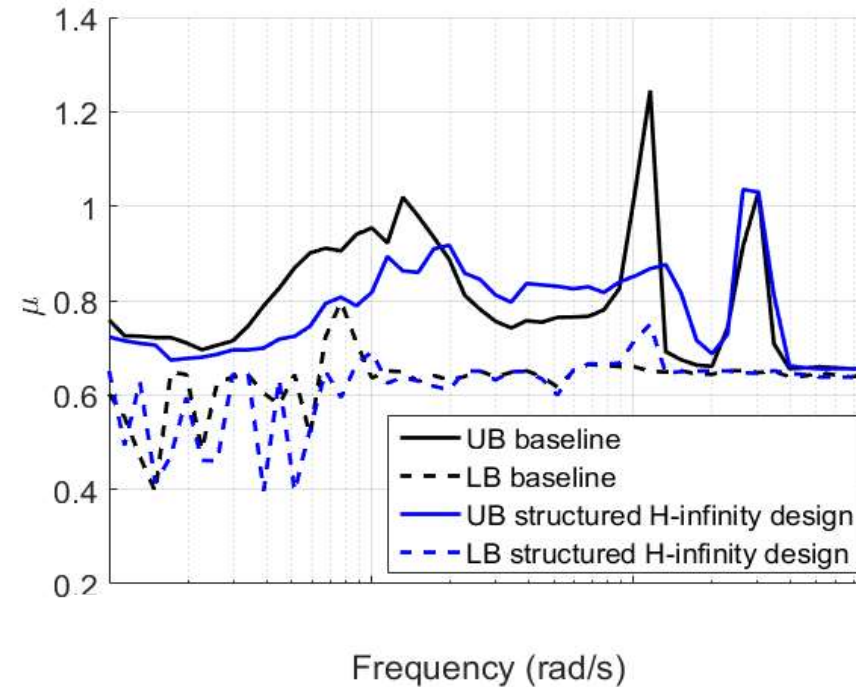
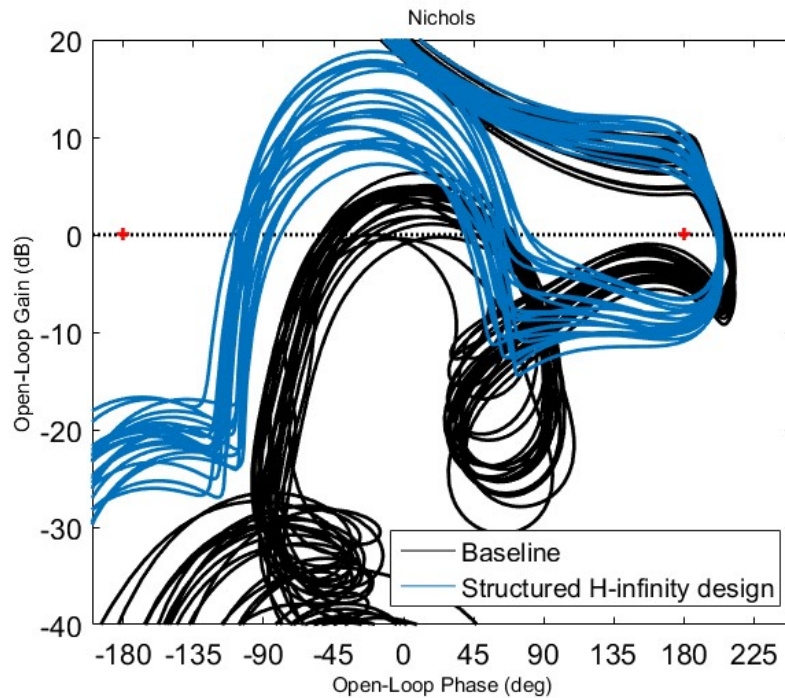
$$H_3 = \prod_{i=1}^2 \frac{s^2 + 2\zeta_{ni}w_{ni}s + w_{ni}^2}{s^2 + 2\zeta_{di}w_{ni}s + w_{ni}^2} \left\{ \frac{s^2 + 2 \cdot 0.24 \cdot 25 \cdot s + 25^2}{s^2 + 2 \cdot 0.4 \cdot 25 \cdot s + 25^2} \right\}^3$$



VEGA Structured H_∞ synthesis: Flexible sequential linear analysis

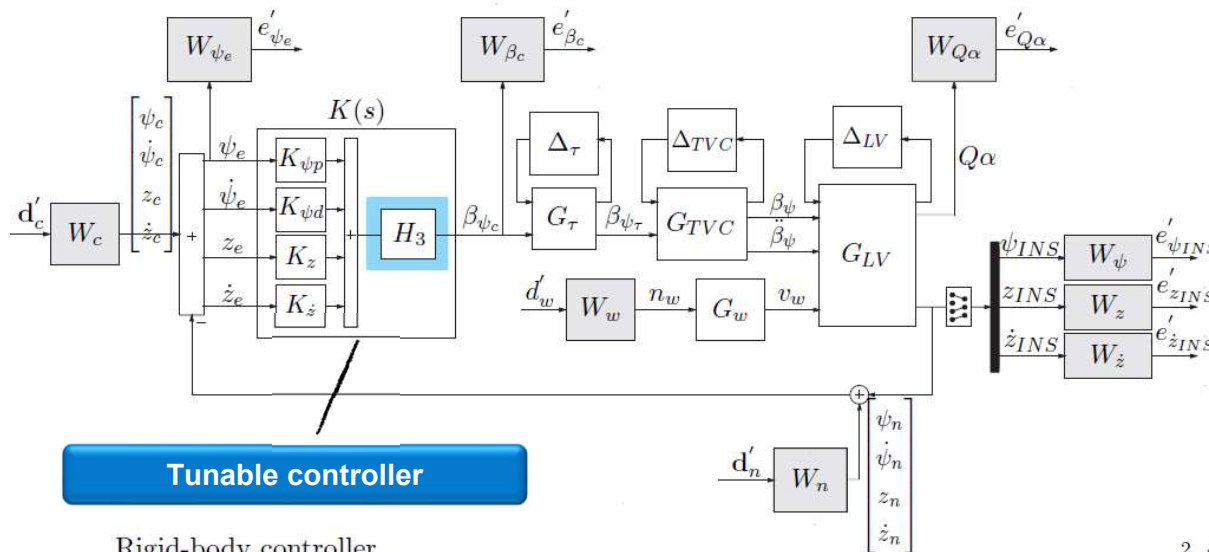
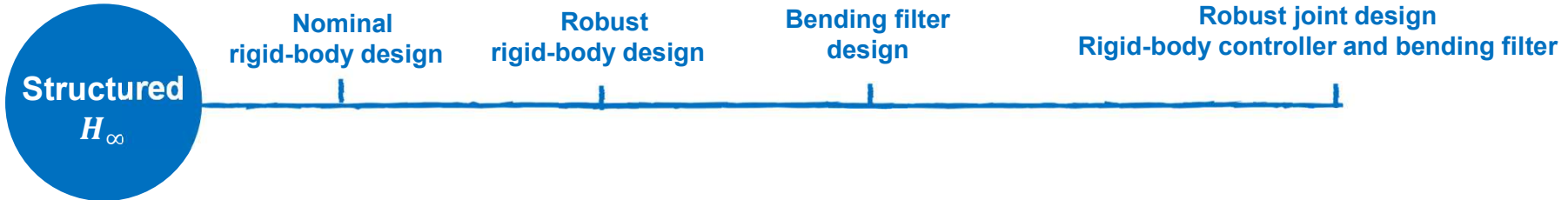


Only 1 linear structured H_∞ controllers is synthesized and analyzed

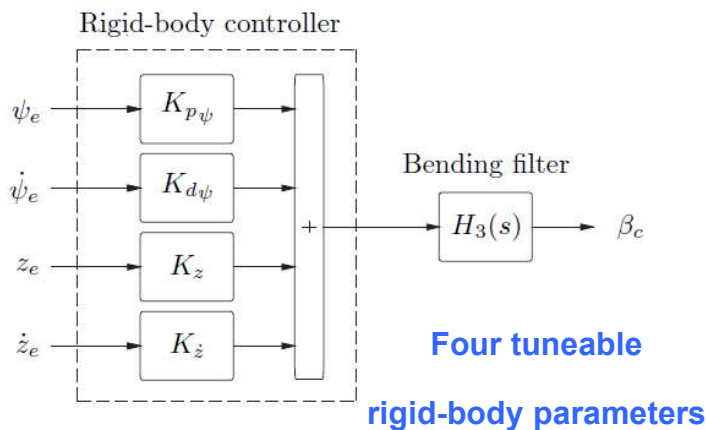


Potential for improvement
with respect to baseline bending filter

VEGA Structured H_∞ synthesis: Rigid+Flexible integrated design



Tunable controller



Four tuneable

flexible-body parameters

Four tuneable

rigid-body parameters

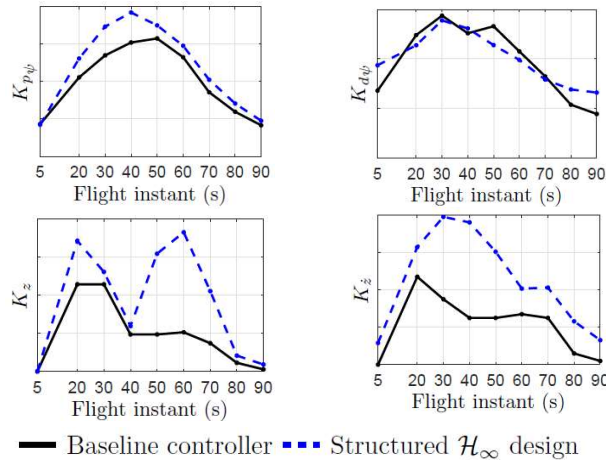
$$H_3(s) = \underbrace{\frac{s^2 + \eta_1 s + (\omega_{q1}')^2}{s^2 + \eta_1/\epsilon_1 s + (\omega_{q1}')^2}}_{\text{Notch filter 1 [min } 1^{st} \text{ BM]}} \underbrace{\frac{s^2 + \eta_2 s + (\omega_{q1})^2}{s^2 + \eta_2/\epsilon_2 s + (\omega_{q1})^2}}_{\text{Notch filter 2 [nom } 1^{st} \text{ BM]}} \underbrace{\frac{s^2 + \eta_3 s + (\overline{\omega_{q1}}')^2}{s^2 + \eta_3/\epsilon_3 s + (\overline{\omega_{q1}}')^2}}_{\text{Notch filter 3 [max } 1^{st} \text{ BM]}}$$

$$\underbrace{\frac{s^2 + \eta_4 s + (\omega_{q2}')^2}{s^2 + \eta_4/\epsilon_4 s + (\omega_{q2}')^2}}_{\text{Notch filter 4 [min } 2^{nd} \text{ BM]}} \underbrace{\left(\frac{\epsilon_{LPS} s^2 + \eta_{LPS} + (0.6\omega_{q2}')^2}{s^2 + \eta_{LPS} + (0.6\omega_{q2}')^2} \right)^3}_{\text{Low-pass filter [Upper BMs attenuation]}}$$

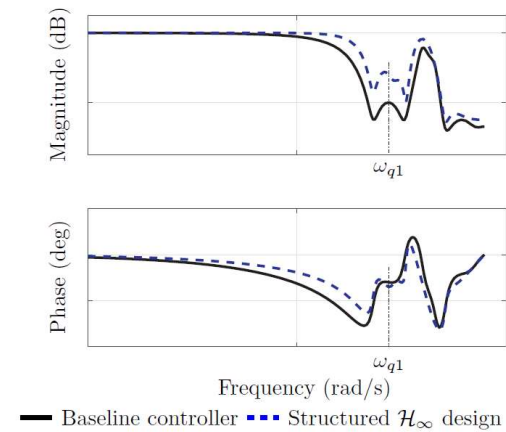
VEGA Structured H_∞ synthesis: Rigid+Flexible integrated analysis

In total, **9 linear integrated structured H_∞ controllers** synthesized along the atmospheric phase

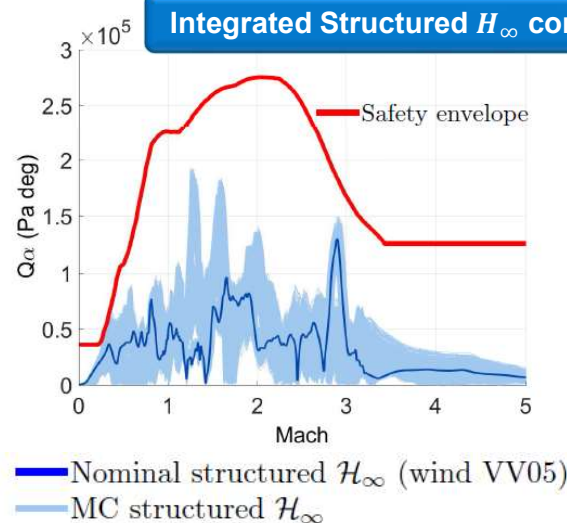
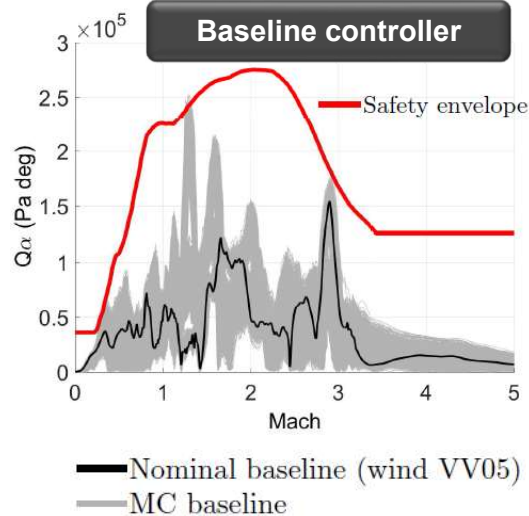
Rigid-body gains



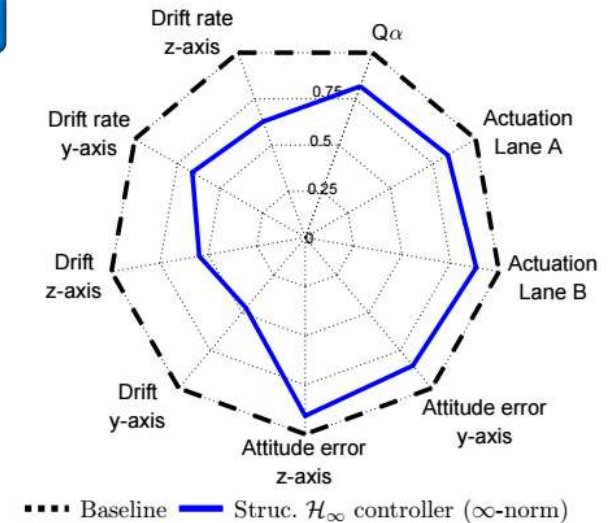
Bending filter comparison at t=50s



Nonlinear Monte Carlo analysis



MC quantitative assessment



Ascent Control:

robust → LPV → Adaptive

VEGA LPV synthesis: Design weighting functions

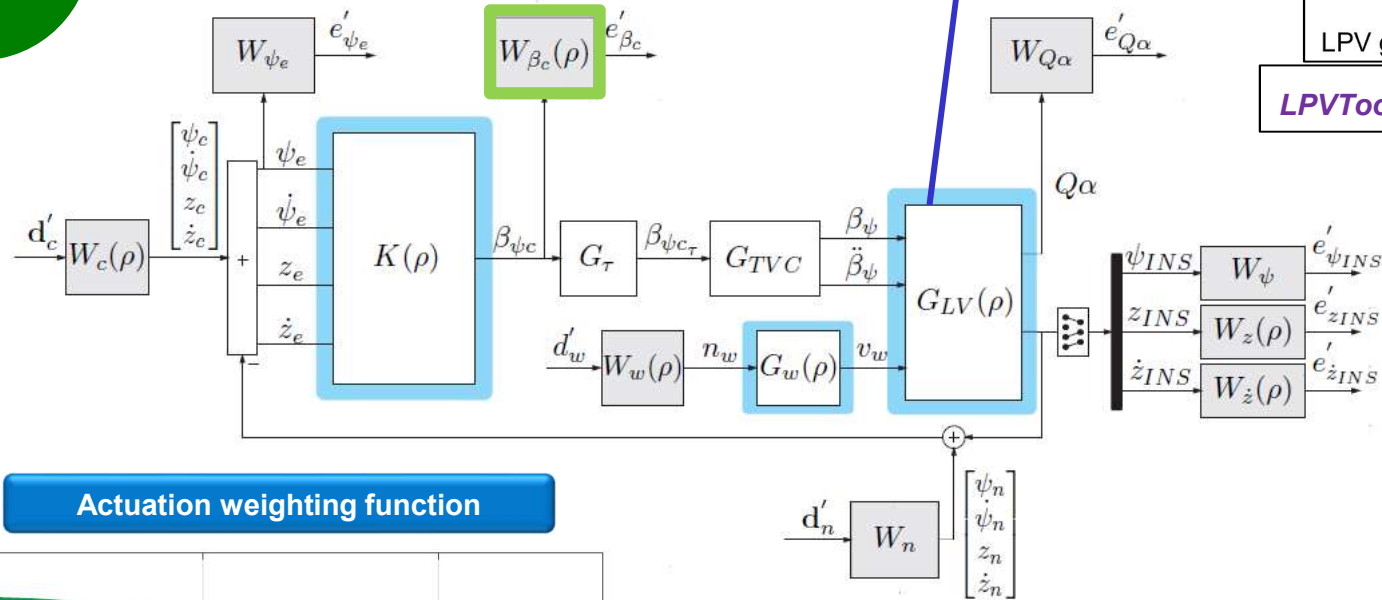
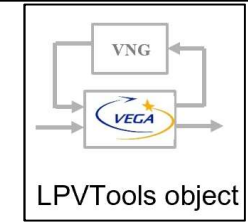
LPV synthesis

$$\begin{bmatrix} \dot{\mathbf{x}}_{LV} \\ \mathbf{u}_{LV} \end{bmatrix} = \underbrace{\begin{bmatrix} A_{LV}(\rho) & B_{LV}(\rho) \\ C_{LV}(\rho) & D_{LV}(\rho) \end{bmatrix}}_{G_{LV}(s,\rho)} \begin{bmatrix} \mathbf{x}_{LV} \\ \mathbf{y}_{LV} \end{bmatrix}; \quad \text{with } \rho(t) \in \mathcal{P}_{NGV} \\ \underline{\nu}_{NGA} < \dot{\rho}(t) < \overline{\nu}_{NGA}$$

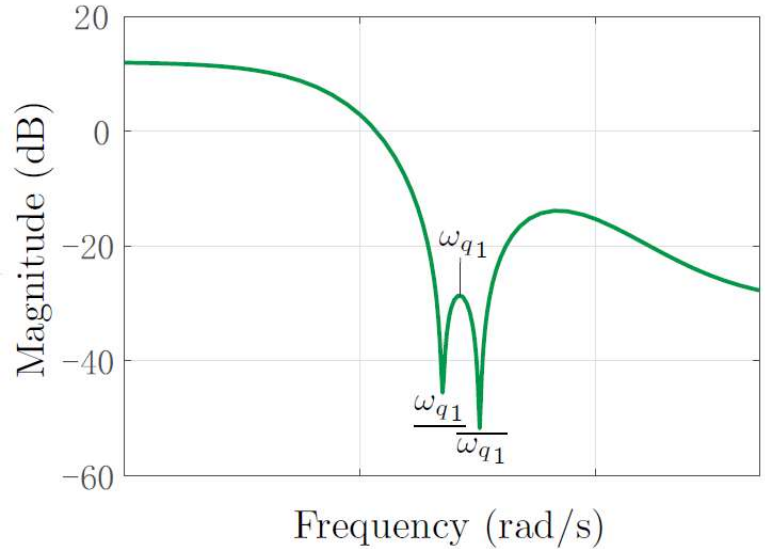


LPV grid: $t = [20 \ 40 \ 50 \ 60 \ 70 \ 90]s$

LPVTools1.0 toolbox from UMN



Actuation weighting function



$$W_u^{-1}(s, \theta) = \underbrace{\frac{s^2 + 0.5s + (\omega_{q1}(\theta))^2}{s^2 + 70s + (\omega_{q1}(\theta))^2}}_{\text{Notch 1}} \underbrace{\frac{s^2 + 0.5s + (\overline{\omega_{q1}}(\theta))^2}{s^2 + 70s + (\overline{\omega_{q1}}(\theta))^2}}_{\text{Notch 2}} \underbrace{F(s, \theta)}_{\text{Low-pass filter}}$$

LPV synthesis

LPV synthesis using *LPVTools1.0 toolbox* from UMN

Control problem formulated as: $\min_{K(s,\rho)} \|\mathcal{T}_{e'd'}(s,\rho)\|_{\mathcal{L}_2 \rightarrow \mathcal{L}_2}$; subject to $\rho(t) \in \mathcal{P}_{NGV}$
 $\underline{\nu}_{NGA} < \dot{\rho}(t) < \overline{\nu}_{NGA}$

Quadratic basis functions to constrain the rate variation of VNG:

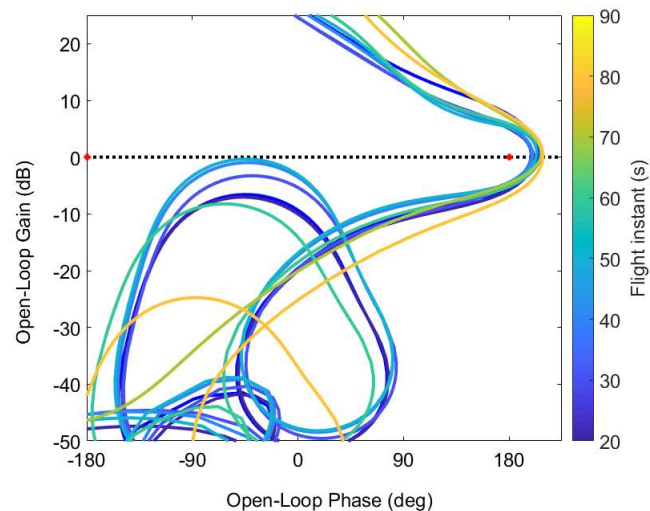
$$X_\rho = X_0 + X_1\rho + X_2\rho^2$$

$$Y_\rho = Y_0 + Y_1\rho + Y_2\rho^2$$

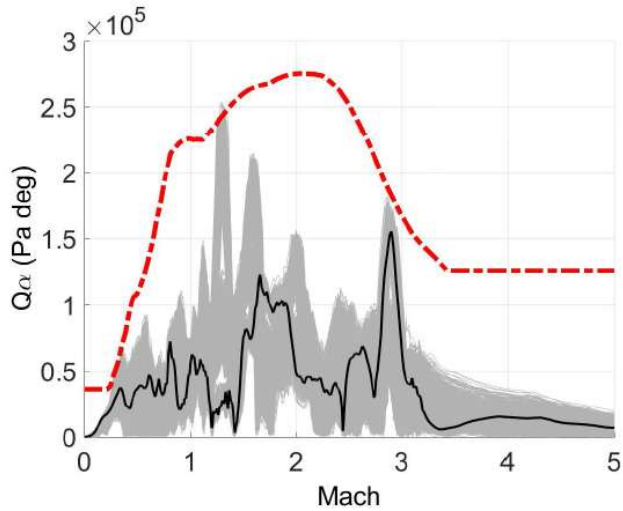
High computational complexity

Resultant controller (rigid-body and bending filter): **22 states**

V&V Stability

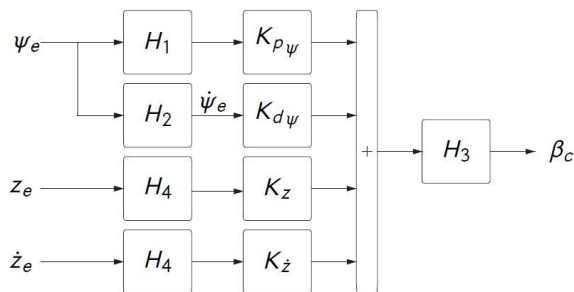


Baseline

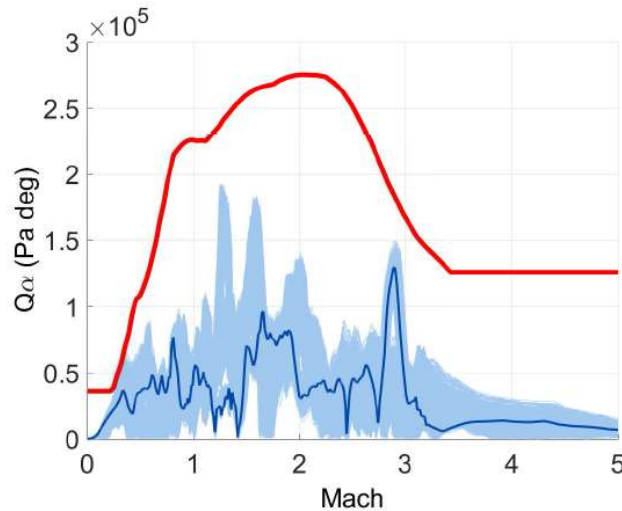


4 gains

23 states controller

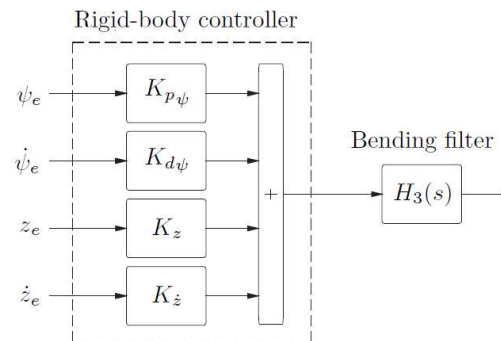


Integrated RigFlex Structured H_∞

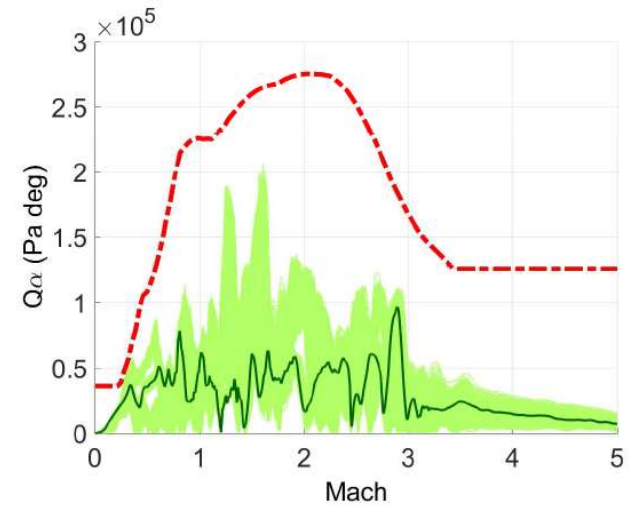


4 gains

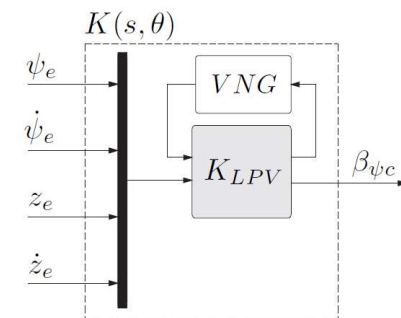
15 states controller



LPV



Full-order controller: 22 states



VEGA Structured H_∞ +IM synthesis: Additional controller structure

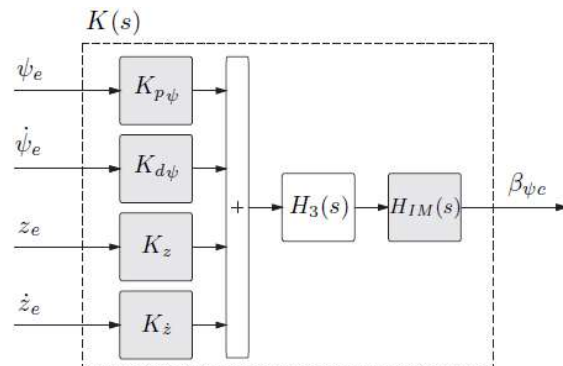
Structured H_∞ design improves robustness & performance for same controller structure

➔ better gain-tunings are possible (and in an easier and more methodological manner)

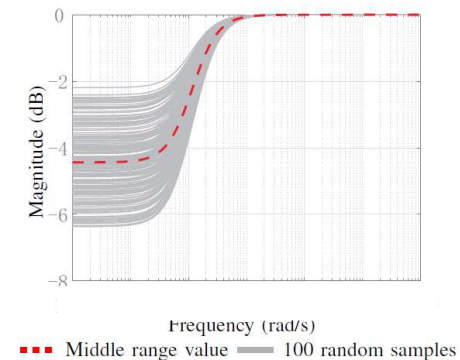
Non-Rate Bounded LPV design shows that there is room to improve robustness and performance

➔ better controller architectures can, and should, be used

Redesign the **integrated structured H_∞** controller including an identified **internal model $H_{IM}(s)$**



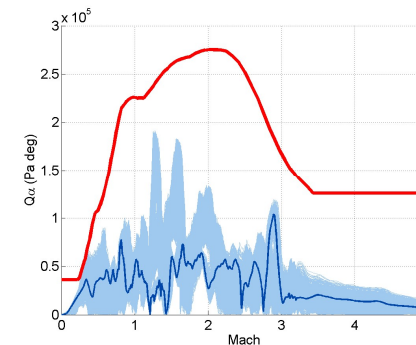
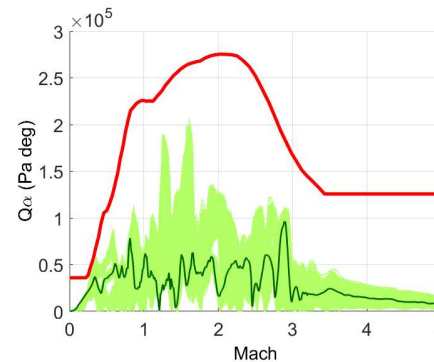
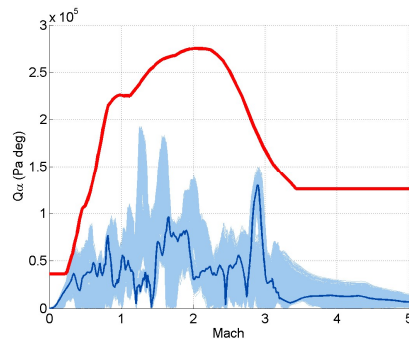
$H_{IM}(s)$
1st-order high-pass TF
with tuneable
pole and zero parameters



Structured H_∞

LPV

Structured H_∞ with Internal Model



Ascent Control:

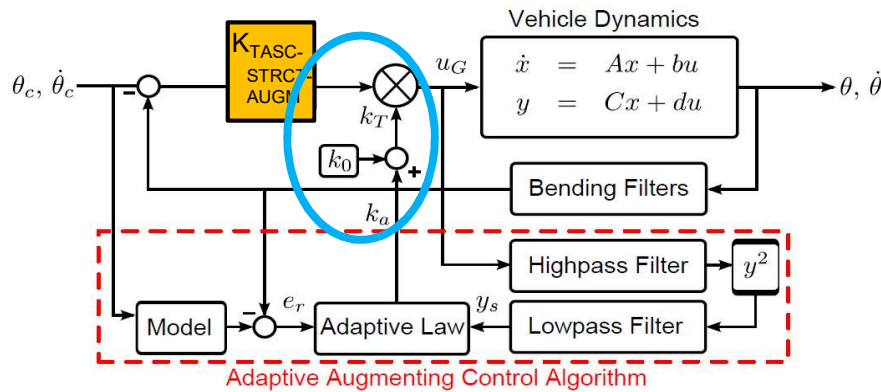
robust → LPV → Adaptive

LPV versus Adaptive control: NASA adaptive controllers description

ADAPTIVE CONTROL LAW – A (2012)

J. Orr and T.S. VanZwieten
 “Robust, Practical Adaptive Control for Launch Vehicles”,
 in AIAA Guidance, Navigation, and Control Conference, 2012

Adaptive augmentation is based on a multiplicative law:



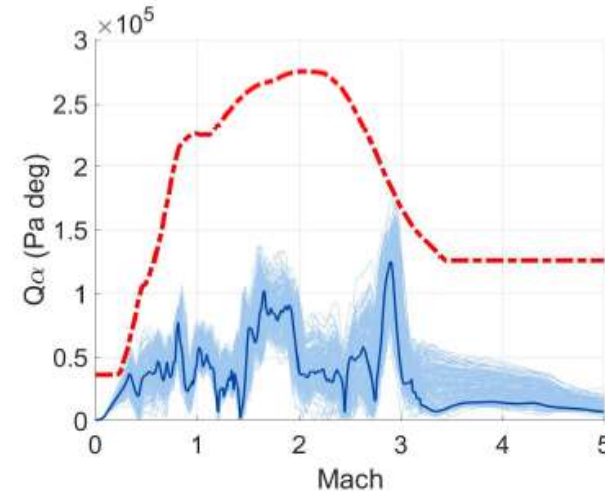
$$k_T = k_0 + k_a$$

Total loop gain
Minimum total loop gain
Adaptive gain

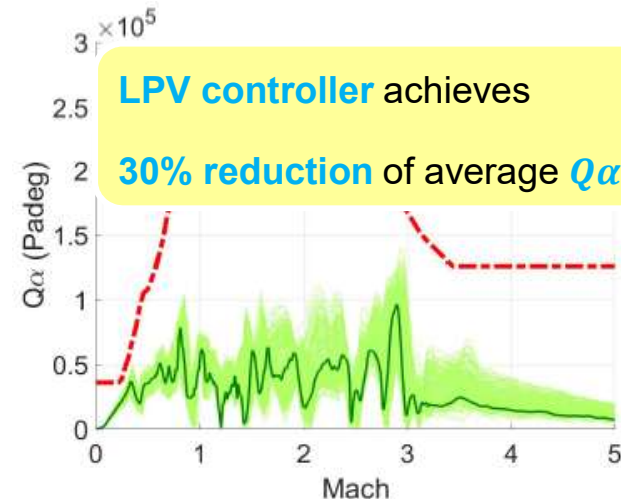
Adaptive gain k_a is given by a first order ODE equation:

$$\dot{k}_a = \underbrace{ae_r^2}_{\text{Adaptive Error}} - \underbrace{\frac{k_a}{k_{max}} ae_r^2}_{\text{Logistic Damper}} - \underbrace{\alpha k_a y_s}_{\text{Spectral Damper}} - \underbrace{\beta(k_T - 1)}_{\text{Leakage}}$$

Adaptive + integrated structured H_∞



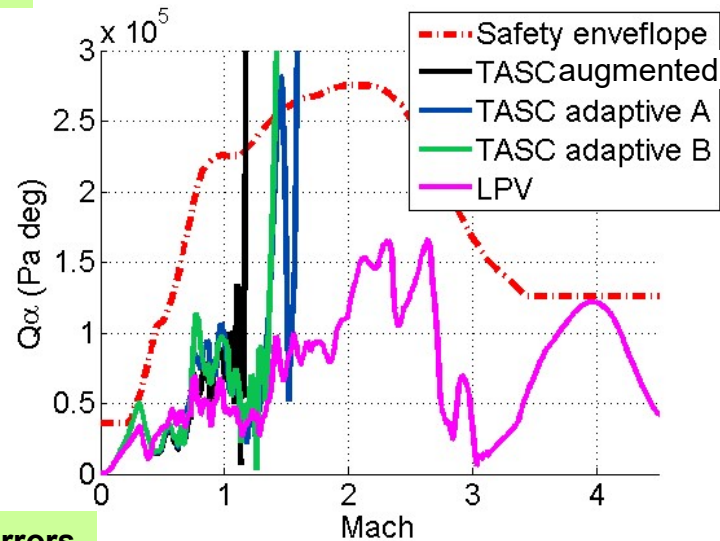
LPV



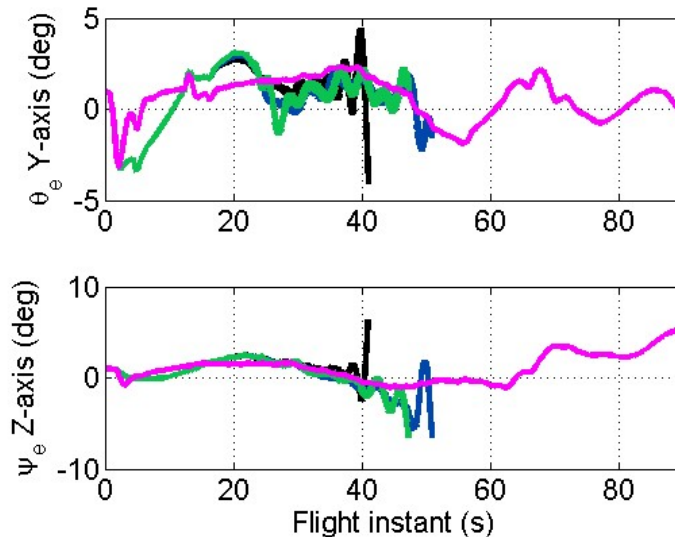
LPV controller achieves
 30% reduction of average Q_α peaks

LPV versus Adaptive control: Test case #5⁺ – performance

Q_α



Attitude errors



Test case #5⁺

- VV05 wind
- All VEGACONTROL flags to **+1.70**

None of adaptive control laws can avoid the loss of vehicle under such extreme conditions

The rate-bounded LPV design still capable of completing mission

- The atmospheric phase *VEGA launcher control design* has been formulated as a robust control problem using
 - **Structured H_∞** (incremental from robust rigid to rigid/flexible integrated design)
 - **LPV**
 - **Adaptive**
- Clear benefits shown for each technique over traditional design
- Use of robust modeling and analysis (LFT & μ) shown to be very advantageous
- **LPV** shown to be best (for the presented case) in terms of:
 - exploitation of robustness and performance domain
 - methodological design approach
 - ease of analysis (especially compared to adaptive)

Marcos, A., Rosa, P., Roux, C., Bartolini, M., Bennani, S., “**An overview of the RFCS project V&V framework: optimization-based and linear tools for worst-case search,**” CEAS Space Journal, June 2015, Volume 7, Issue 2, pp 303-318

Simplício, P., Bennani, S., Lefort, X., Marcos, A., Roux, C., “**Structured Singular Value Analysis of the VEGA Launcher in Atmospheric Flight,**” AIAA Journal of Guidance, Control, and Dynamics, vol. 39, no. 6, pp. 1342-1355, June 2016

Marcos, A., Roux, C., Bennani, S., “**Stochastic mu-Analysis for launcher thrust vector control systems,**” 3rd CEAS EURO-GNC, Toulouse, France, April 2015

Marcos, A., Bennani, S., Roux, C., Valli, M., “**Uncertainty Modeling and Robust Analysis of Atmospheric Launchers: Incremental Steps for Industrial Transfer,**” 8th IFAC Symposium on Robust Control Design (ROCOND), Bratislava, Slovakia, July 2015

Marcos, A., Bennani, S., Roux, C., “**LPV modeling and LFT Uncertainty Identification for Robust Analysis: application to the VEGA Launcher during Atmospheric Phase,**” 1st IFAC Workshop on Linear Parameter Varying Systems, Grenoble, France, October 2015

Navarro-Tapia, D., Marcos, A., Bennani, S., Roux, C., “**Structured H-infinity Control Based on Classical Control Parameters for the VEGA Launch Vehicle,**” IEEE Multi-Conference on Systems and Control (MSC 2016), Buenos Aires, Argentina, September 2016

Navarro-Tapia, D., Marcos, A., Bennani, S., Roux, C., “**Structured H-infinity Control Design for the VEGA Launch Vehicle: Recovery of the Legacy Control Behaviour,**” ESA Guidance, Navigation and Control Conference (ESAGNC 2017), Salzburg, Austria, May 2017

Navarro-Tapia, D., Marcos, A., Bennani, S., Roux, C., “**Structured H_∞ and Linear Parameter Varying control design for the VEGA Launch Vehicle,**” 7th European Conference for Aeronautics and Space Sciences (EUCASS 2017), Milan, Italy, July 2017

Navarro-Tapia, D., Marcos, A., Bennani, S., Roux, C., “**Linear Parameter Varying Control Synthesis for the atmospheric phase VEGA launcher,**” 2nd LPVS symposium, Florianopolis, Brazil, 2018

Navarro-Tapia, D., Marcos, A., Bennani, S., Roux, C., “**Structured H-infinity Control Design for the VEGA Launcher: Robust Control Design Augmentation,**” International Astronautical Congress (IAC), Bremen, Germany, October 2018

Navarro-Tapia, D., Marcos, A., Bennani, S., Roux, C., “**Reconciling Full-Order LPV Design and Augmented Structured H_∞ via Internal Model Principle: A Launcher Application,**” IEEE 7th International Conference on Systems and Control (ICSC), Valencia, Spain, October 2018

Navarro-Tapia, D., Marcos, A., Bennani, S., Roux, C., “**Robust-Control-Based Design and Comparison of an Adaptive Controller for the VEGA Launcher,**” AIAA SciTech, San Diego, USA, Jan. 2019

Descent Guidance: convex pinpoint landing optimization

ESA NPI contract 4000119571/17/NL/MH

“Advanced Flight Control System Design With Active Load & Relief Capabilities”



Samir Bennani



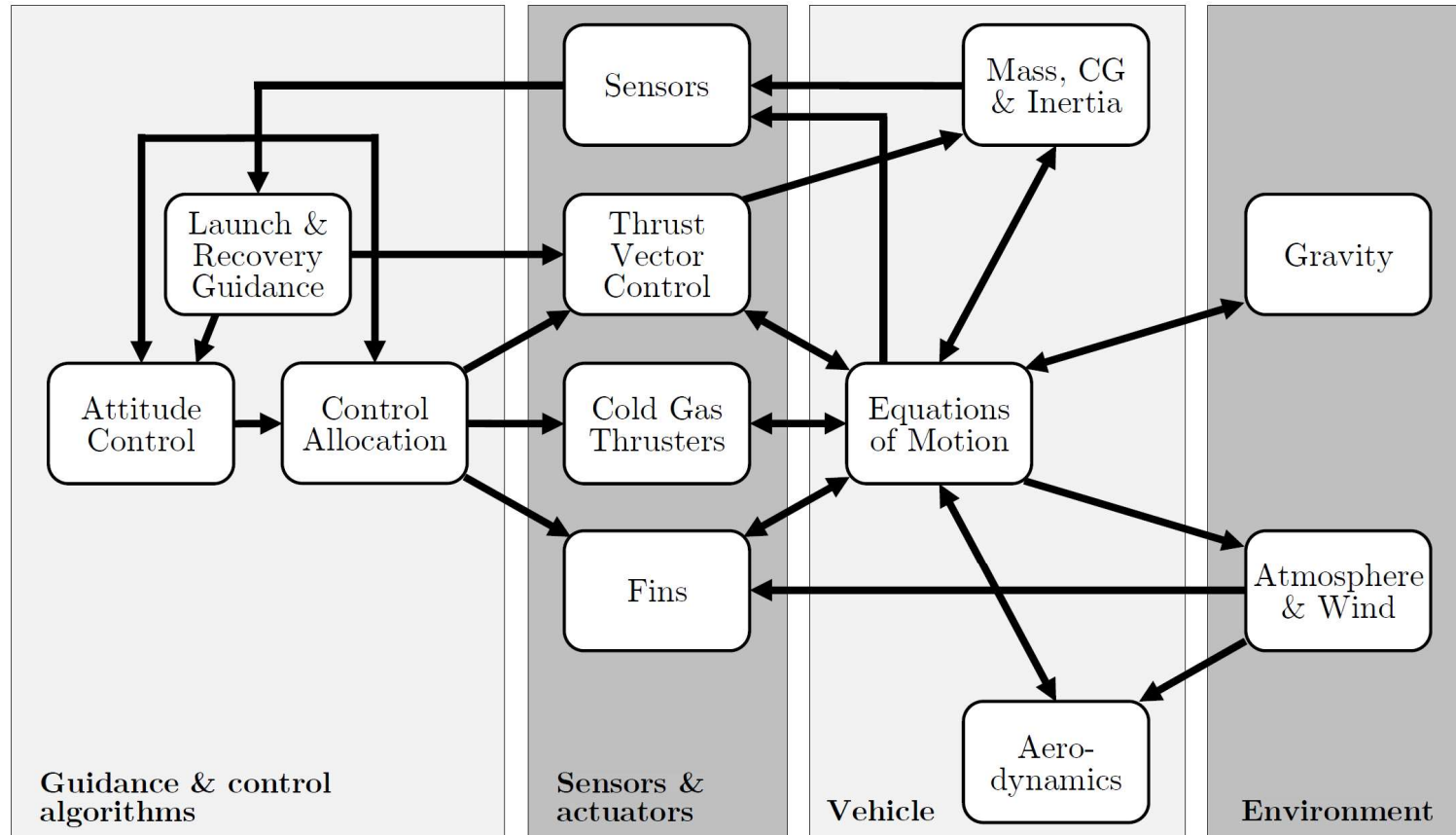
Pedro Simplicio
Andrés Marcos



Stephan Theil
David Seelbinder

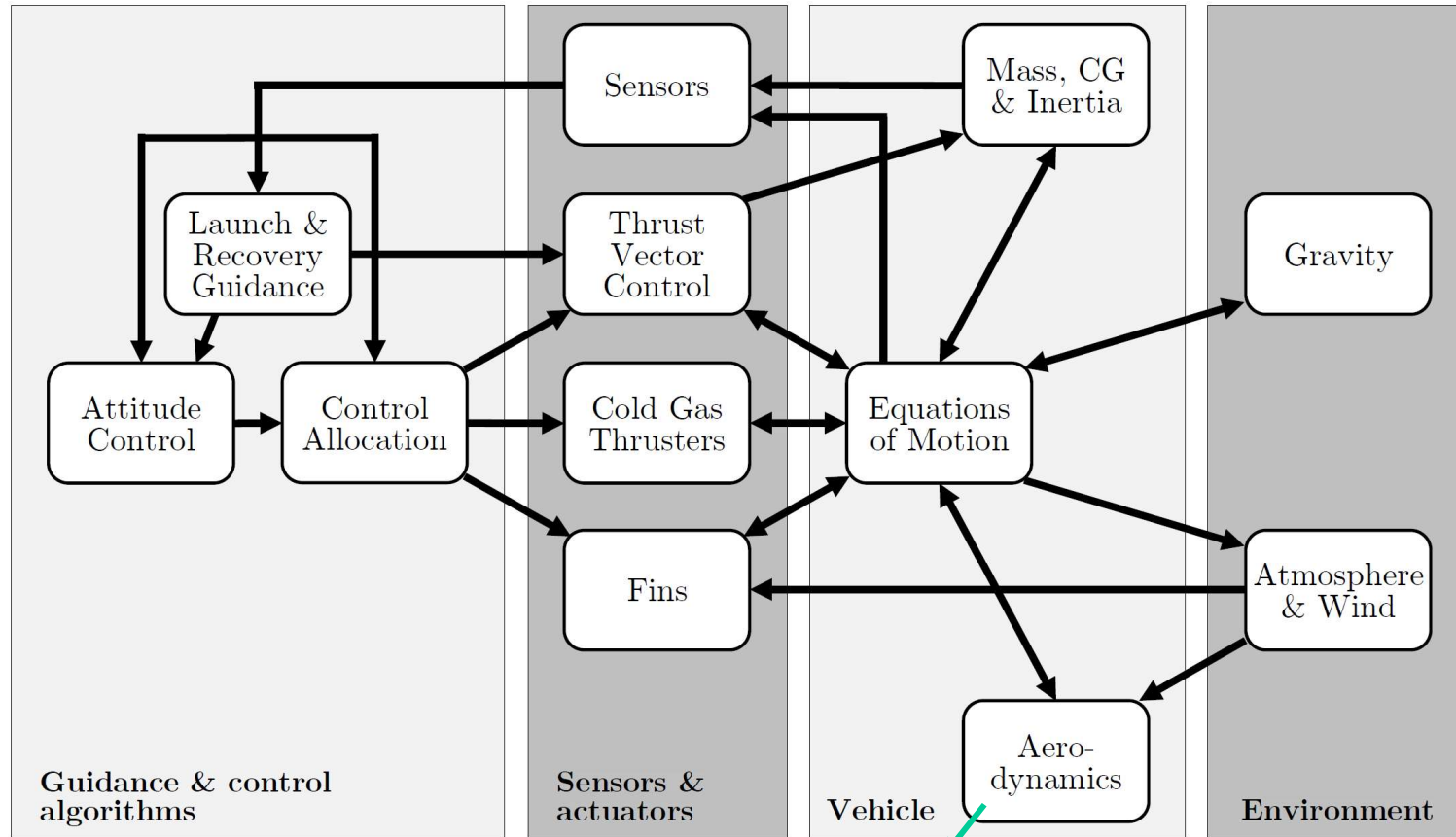


Descent Guidance: Reusable launcher model



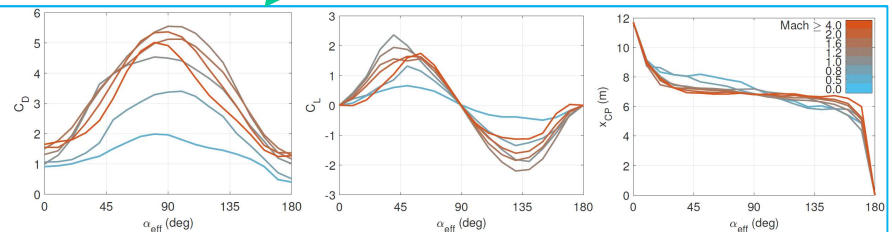


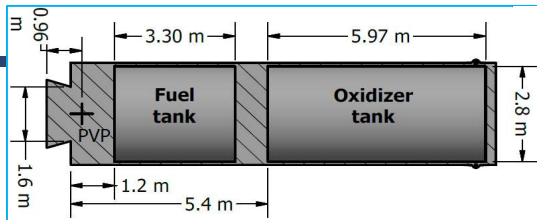
Descent Guidance: Reusable launcher model



VEGA-like aerodynamics based on ascent and post-separation data*

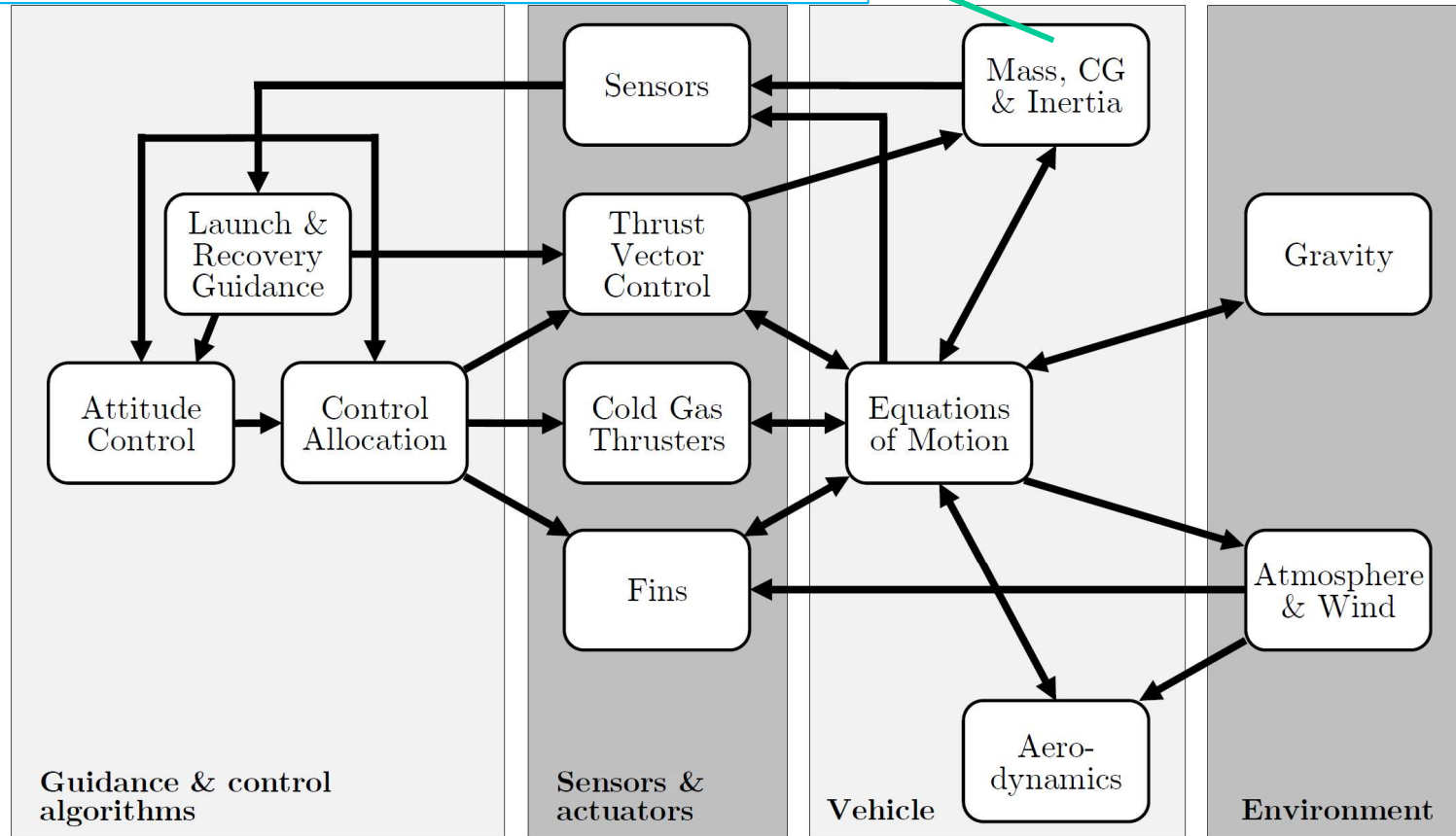
*kindly provided by ELV/Avio



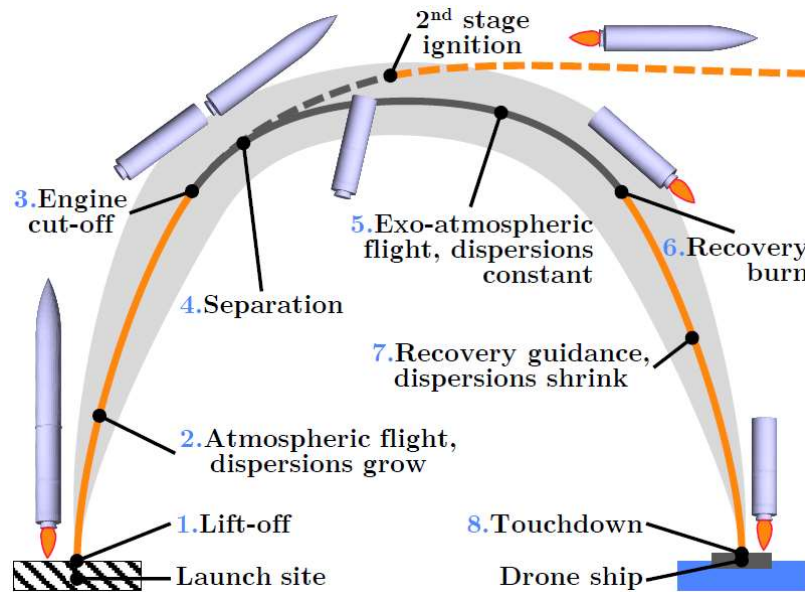


MCI updated online based on LOX/RP-1 re-ignitable engine

Descent Guidance: Reusable launcher model

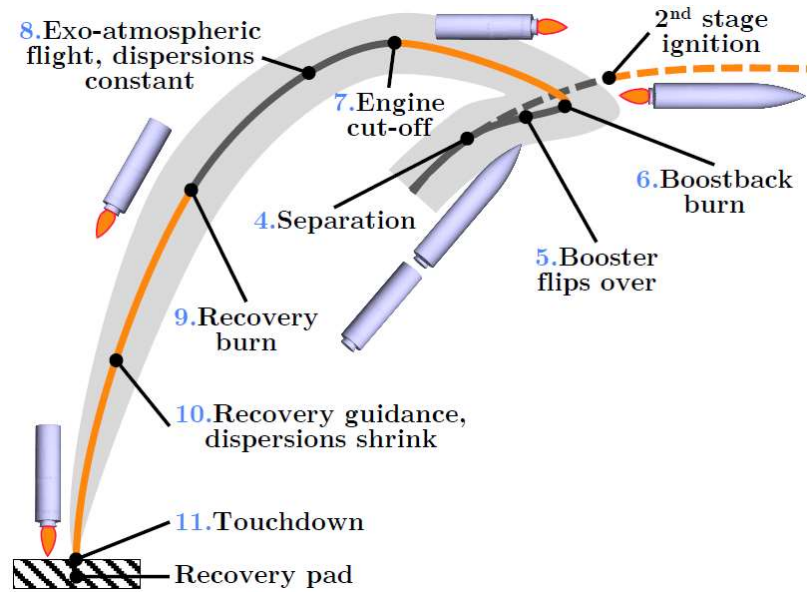


Downrange landing (DRL)



 Recovery: 5.5% of launch

Return to launch site (RTLS)



 Recovery: 10.6% of launch

Need to shrink dispersions for pinpoint landing requires closed-loop guidance algorithms

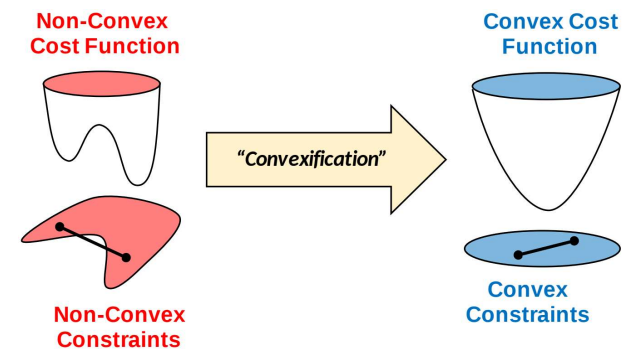
➤ Constrained terminal velocity

- Closed-form solution of a **simplified fuel-optimal** control problem
- Simple but **unable** to enforce path constraints

$$\mathbf{T}_{CTV}(t) = \hat{m}(t) \begin{bmatrix} k_r & k_v \end{bmatrix} \begin{bmatrix} \frac{\mathbf{ZEM}(t)}{(t_f - t)^2} \\ \frac{\mathbf{ZEV}(t)}{t_f - t} \end{bmatrix}$$

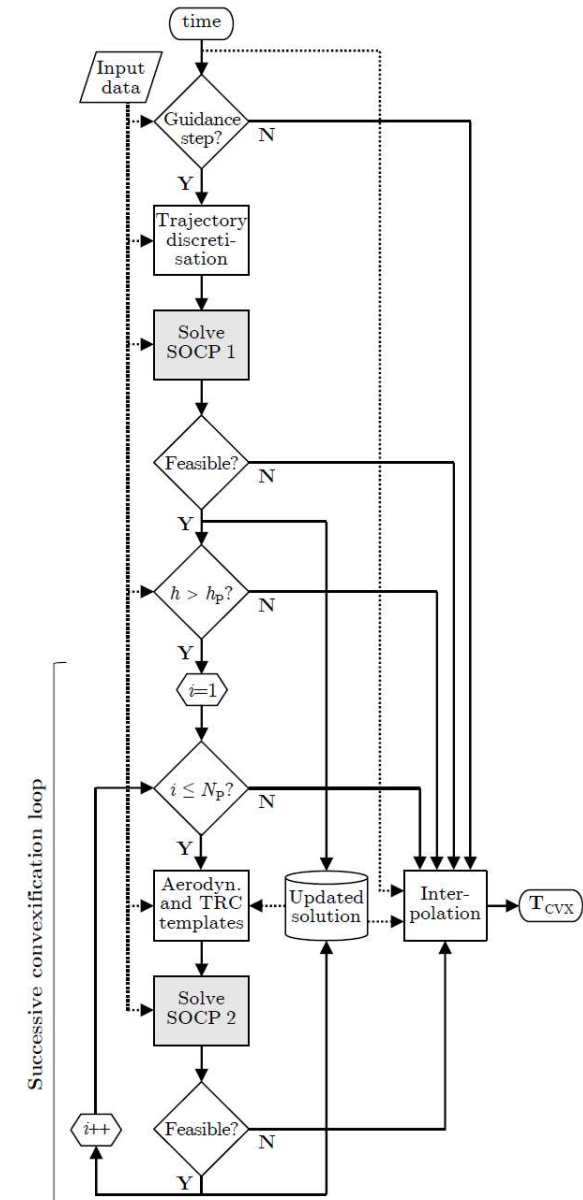
➤ Convex optimisation-based

- Recovery trajectory and thrust commands updated on-board
- Real-time **reliable** via convexification of the constrained optimal control problem
- **Novel algorithm** developed to cope with the extended flight envelope of RLVs



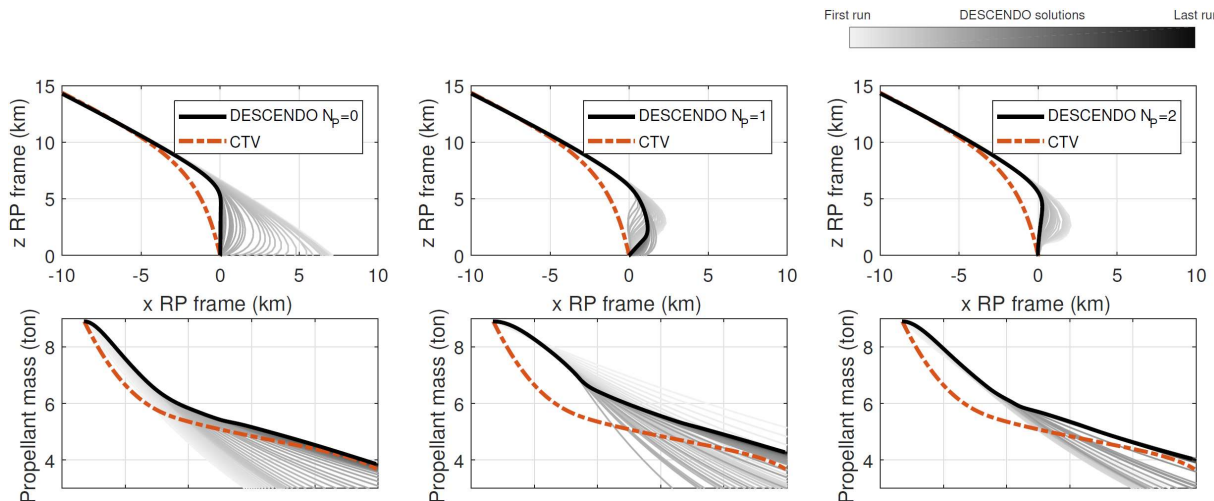
Descending over Extended Envelopes using Successive Convexification-based Optimisation

- At each simulation instance, commands are interpolated from most recent guidance solution
- Solution updated once a SOCP is triggered and feasible
- SOCP 1** finds a **discrete trajectory** that does not account for aerodynamic forces
- SOCP 2** applies **successive convexification** to approximate these forces



Descending over Extended Envelopes using Successive Convexification-based Optimisation

- At each simulation instance, commands are interpolated from most recent guidance solution
- Solution updated once a SOCP is triggered and feasible
- SOCP 1** finds a **discrete trajectory** that does not account for aerodynamic forces
- SOCP 2** applies **successive convexification** to approximate these forces



SOCP 2

$$\max_{\mathbf{w}, \sigma} z[N] - w_{\eta_w} \sum_{k=1}^N \eta_w[k], \quad \text{subject to:}$$

Boundary conditions

$$z[1] = \ln \hat{m}(t), \quad \mathbf{r}[1] = \hat{\mathbf{r}}(t), \quad \mathbf{v}[1] = \hat{\mathbf{v}}(t), \quad \mathbf{w}[1] = \hat{\mathbf{w}}(t)$$

$$\mathbf{r}[N] = \mathbf{r}_f, \quad \mathbf{v}[N] = \mathbf{v}_f, \quad \mathbf{w}_{x,y}[N] = \mathbf{0}_{2 \times 1}, \quad w_z[N] \geq 0$$

Dynamics equations, $\forall k \in [1, \dots, N-1]$

$$\mathbf{r}[k+1] = \mathbf{r}[k] + T_S \mathbf{v}[k] + \frac{T_S^2}{3} \left(\mathbf{a}[k] + \frac{\mathbf{a}[k+1]}{2} \right)$$

$$\mathbf{v}[k+1] = \mathbf{v}[k] + \frac{T_S}{2} (\mathbf{a}[k] + \mathbf{a}[k+1])$$

$$z[k+1] = z[k] - \frac{1}{I_{sp} g_0} \frac{T_S}{2} (\sigma[k] + \sigma[k+1])$$

Surrogate variables, $\forall k \in [1, \dots, N]$

$$\mathbf{a}[k] = \mathbf{w}[k] + \hat{\mathbf{g}}(t) - d_i^*[k] \mathbf{v}[k]$$

$$\|\mathbf{w}[k]\| \leq \sigma[k]$$

Trust region constraints, $\forall k \in [1, \dots, N]$

$$\|\mathbf{w}[k] - \mathbf{w}_i^*[k]\| \leq \eta_w[k]$$

Flight path constraints, $\forall k \in [1, \dots, N-1]$

$$\mathbf{r}_z[k] \geq \frac{\hat{\mathbf{r}}_z(t)}{\|\hat{\mathbf{r}}_{x,y}(t)\|} \|\mathbf{r}_{x,y}[k]\|$$

Control constraints, $\forall k \in [1, \dots, N-1]$

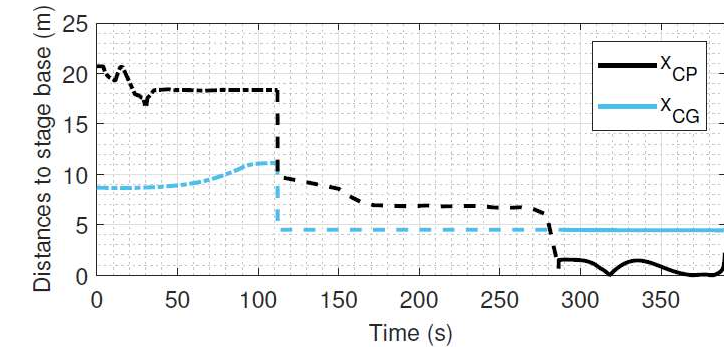
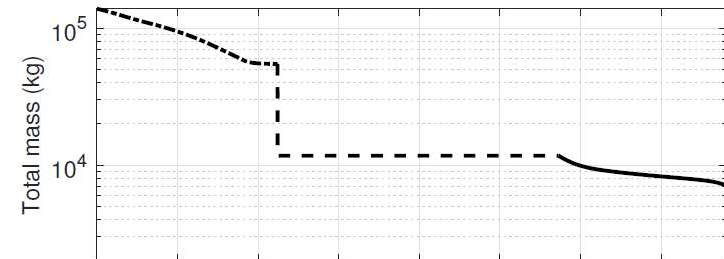
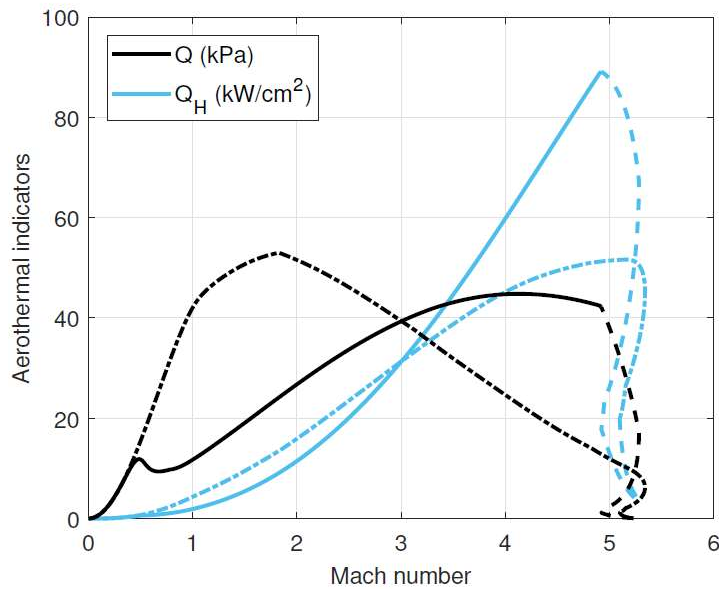
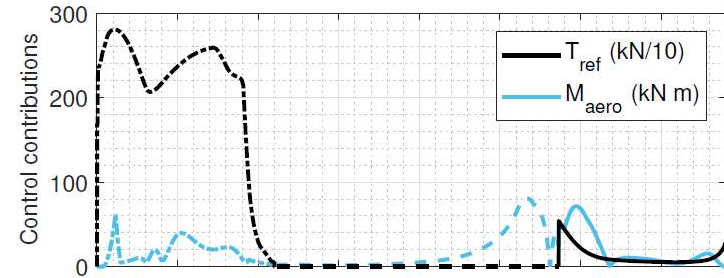
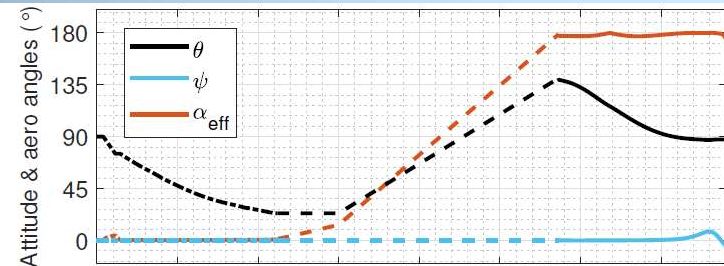
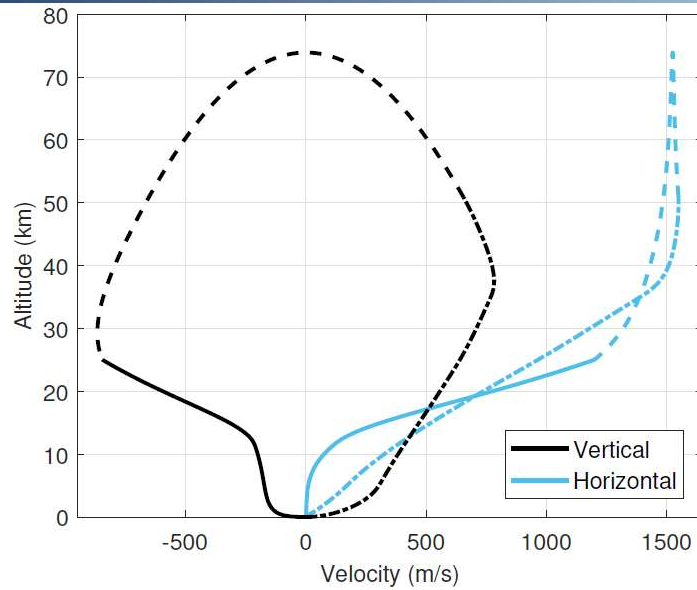
$$\begin{cases} w_z[k] \geq \frac{\|\mathbf{w}_{x,y}[k]\|}{\tan \theta_{\max}}, & \frac{T_{\min}}{\hat{m}(t)} \leq \sigma[k] \leq \frac{T_{\max}}{\hat{m}(t)}, & \text{if } T_S(k-1) \in \mathcal{T}_P \\ \mathbf{w}[k] = \mathbf{0}_{3 \times 1}, & & \text{otherwise} \end{cases}$$

Control rate constraints, $\forall k \in [1, \dots, N-1]$

$$\sigma[k] - T_S \frac{\hat{T}_{\max}}{\hat{m}(t)} \leq \sigma[k+1] \leq \sigma[k] + T_S \frac{\hat{T}_{\max}}{\hat{m}(t)}$$

Descent Guidance:

The DESCENDO algorithm – detailed DRL trajectory results



Simplício, P., Marcos, A., Joffre, E., Zamaro, M., Silva, N., “**Systematic Performance-oriented Guidance Tuning for Descent & Landing on Small Planetary Bodies**,” Acta Astronautica, published online July 2018

Joffre, E., Zamaro, M., Silva, N., Marcos, A., Simplício, P., Richardson, B., “**Trajectory Design and Guidance for Landing on Phobos**,” Acta Astronautica, vol. 151, pp. 389-400, Oct 2018.

Simplício, P., Marcos, A., Joffre, E., Zamaro, M., Silva, N., “**Survey of Guidance Techniques for Planetary Descent**,” Progress in Aerospace Sciences, published online November 2018

Simplício, P., Marcos, A., Bennani, S., “**Guidance of Reusable Launchers: Improving Descent and Landing Performance**,” AIAA Journal of Guidance, Control, and Dynamics, accepted for publication January 2019

Simplício, P., Marcos, A., Joffre, E., Zamaro, M., Silva, N., “**Parameterised Laws for Robust Guidance and Control of Planetary Landers**,” 4th CEAS Specialist Conference on Guidance, Navigation and Control (EuroGNC 2017), Warsaw, Poland, April 2017

Joffre, E., Zamaro, M., Silva, N., Marcos, A., Simplício, P., Richardson, B., “**Results of new guidance and control strategies for landing on small bodies**,” ESA Guidance, Navigation and Control Conference (ESAGNC 2017), Salzburg, Austria, May 2017

Simplício, P., Marcos, A., Joffre, E., Zamaro, M., Silva, N., “**A Systematic Performance-Oriented Tuning for Space Exploration Descent & Landing Guidance**,” 7th European Conference for Aeronautics and Space Sciences (EUCASS 2017), Milan, Italy, July 2017

Simplício, P., Marcos, A., Bennani, S., “**A Reusable Launcher Benchmark with Advanced Recovery Guidance**,” 5th CEAS EuroGNC, Milan, Italy, April 2019

Ascent Load Relief: Wind Disturbance Observer (WDO)

ESA NPI contract 4000119571/17/NL/MH

“Advanced Flight Control System Design With Active Load & Relief Capabilities”



Samir Bennani

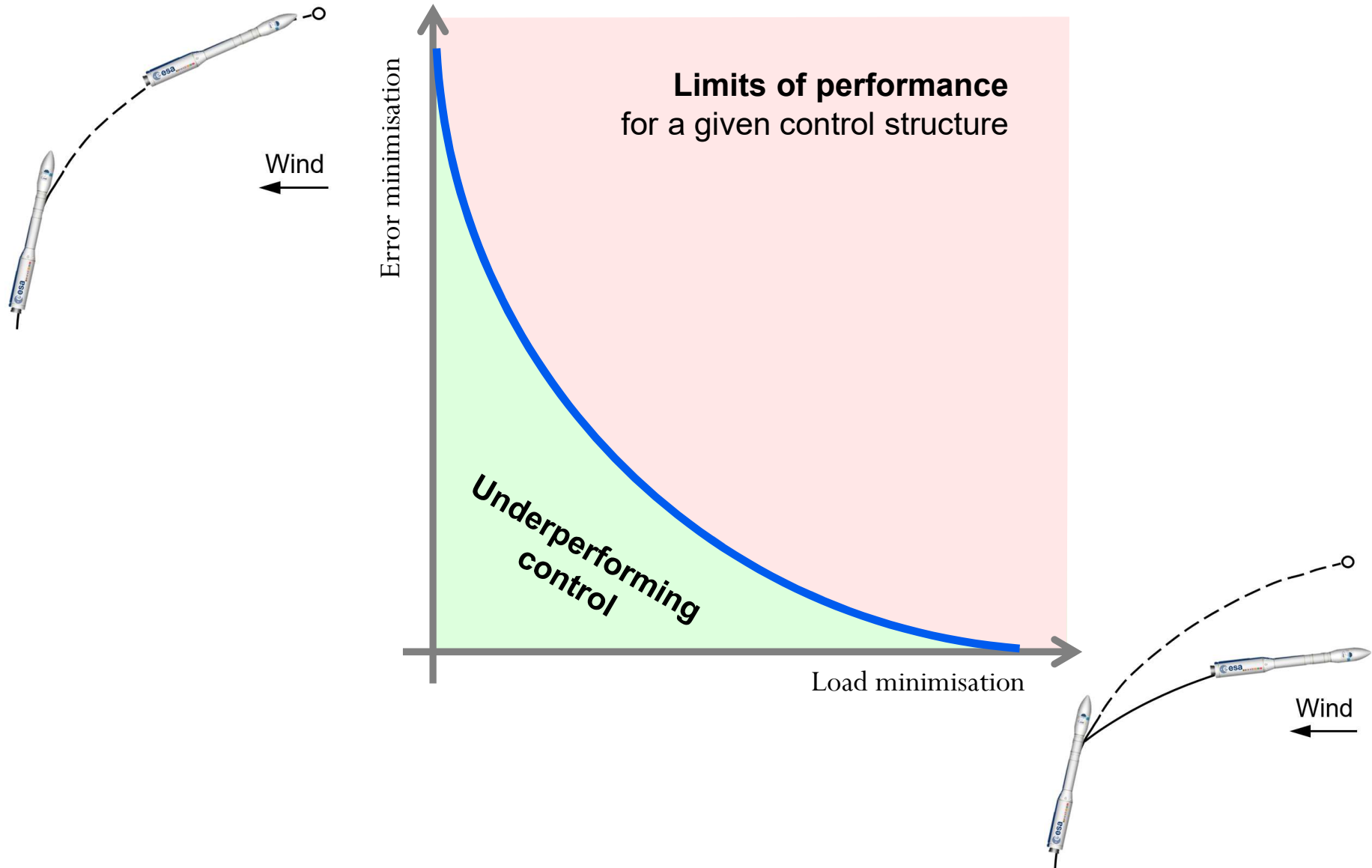


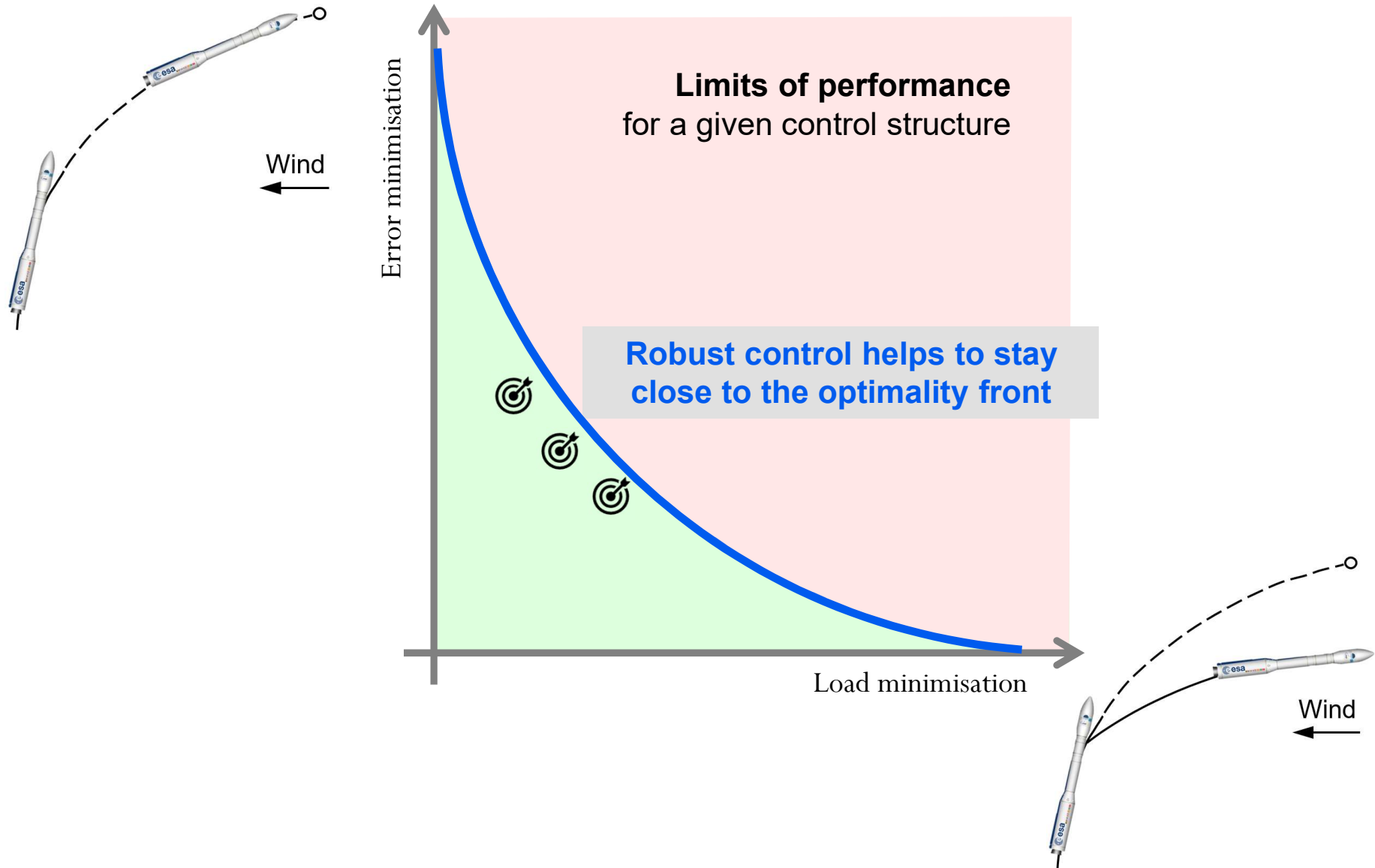
Pedro Simplicio
Andrés Marcos



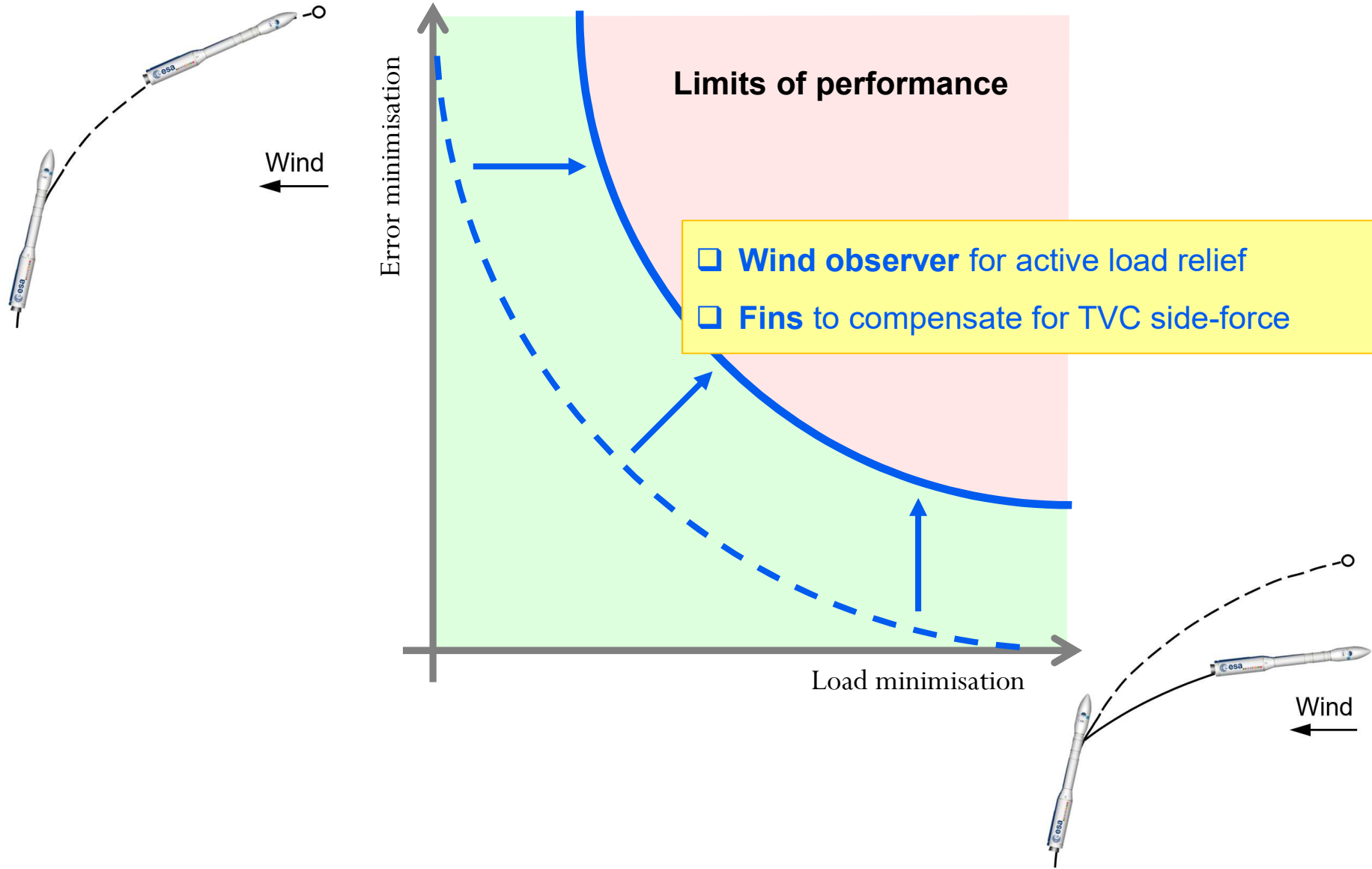
Stephan Theil
David Seelbinder

Ascent Load Relief: Achievable performance





Ascent Load Relief: Achievable performance

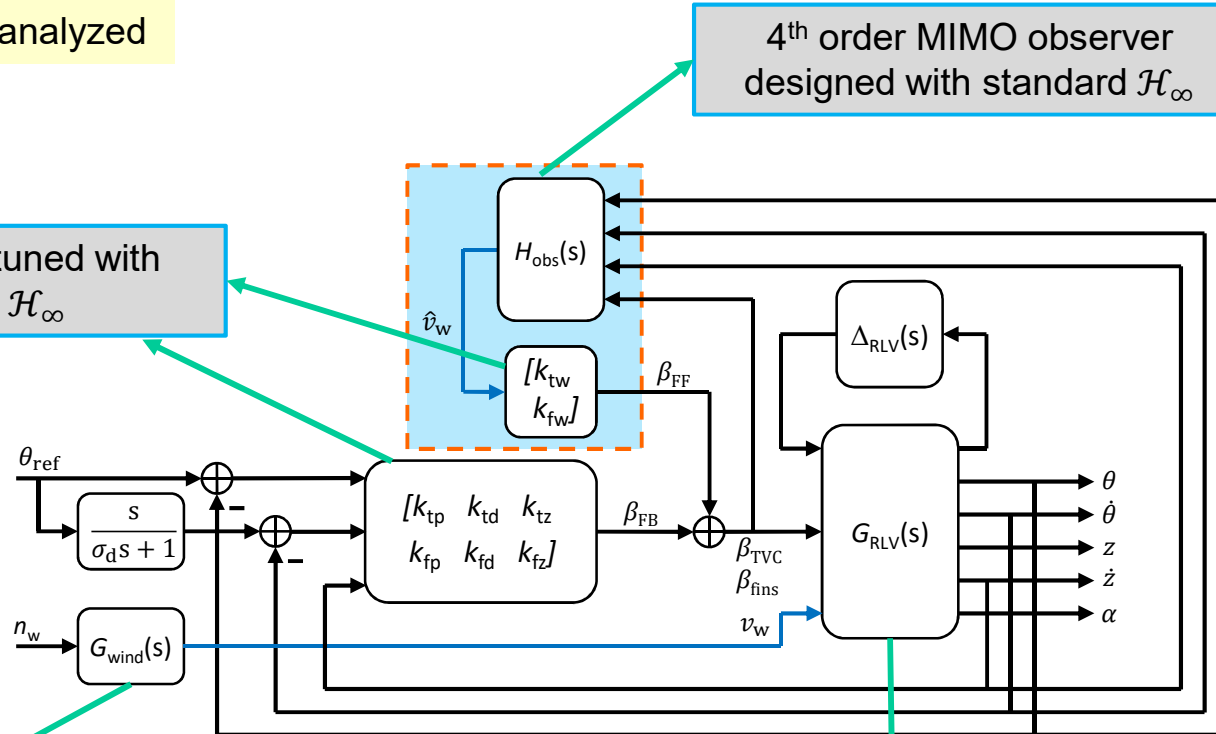


Only 1 linear design is synthesized and analyzed

4th order MIMO observer designed with standard \mathcal{H}_∞

8 control gains tuned with structured \mathcal{H}_∞

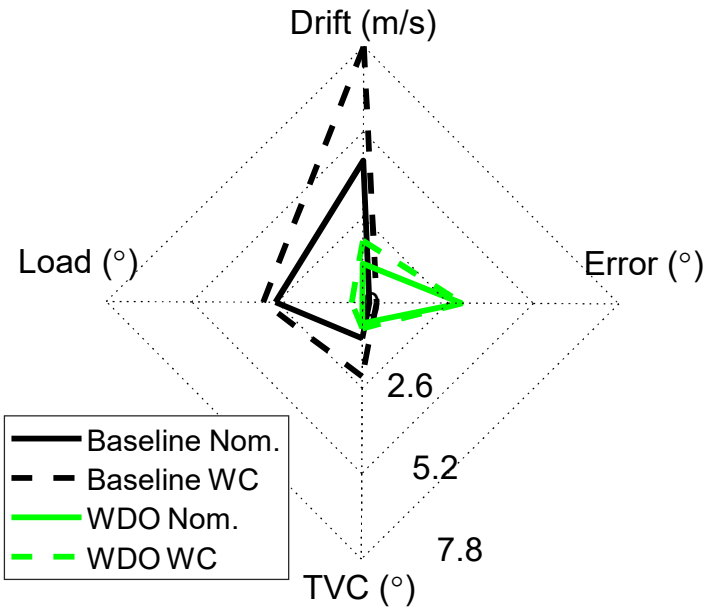
Wind disturbances, with frequency-colouring filter



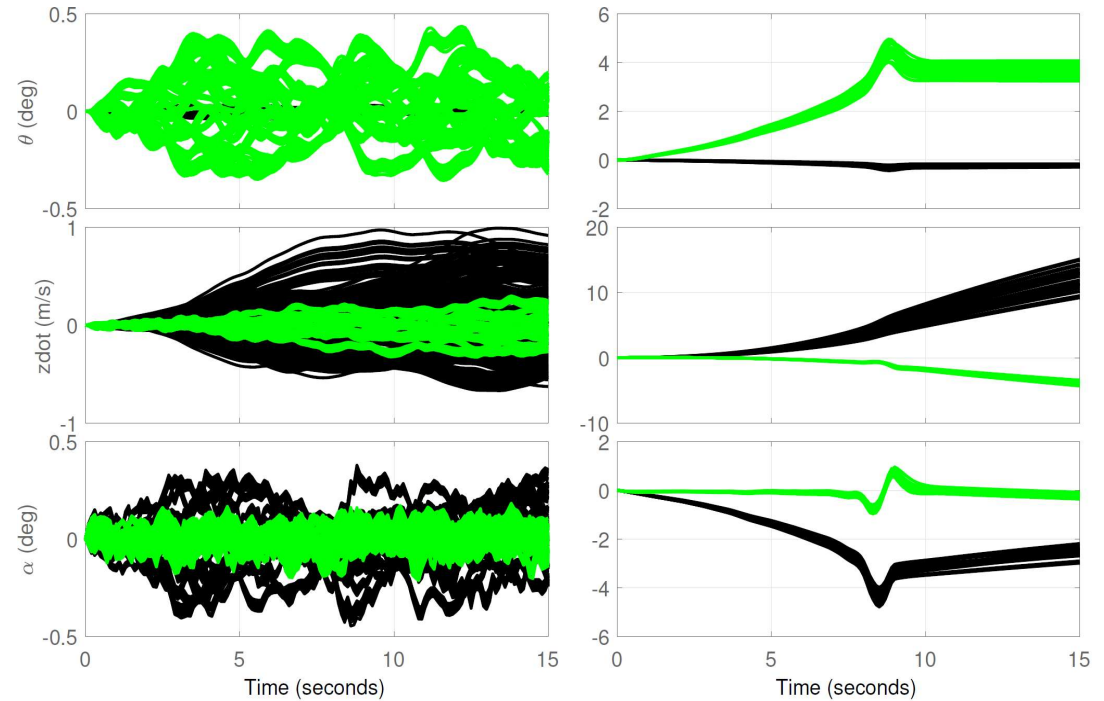
LTI model wrt. different points along trajectory

$$\begin{bmatrix} \dot{\theta} \\ \ddot{\theta} \\ \dot{z} \\ \ddot{z} \end{bmatrix} = \begin{bmatrix} 0 & 1 & 0 & 0 \\ \mu_\alpha + \mu_f & 0 & 0 & \frac{\mu_\alpha + \mu_f}{V \cos \alpha_0} \\ 0 & 0 & 0 & 1 \\ -g \sin \theta_0 - \frac{N_\alpha + N_f}{m} & 0 & 0 & -\frac{N_\alpha + N_f}{mV \cos \alpha_0} \end{bmatrix} \begin{bmatrix} \theta \\ \dot{\theta} \\ z \\ \dot{z} \end{bmatrix} + \begin{bmatrix} 0 & 0 & 0 & 0 \\ -\mu_c & -\mu_f & -\mu_j & -\frac{\mu_\alpha + \mu_f}{V \cos \alpha_0} \\ 0 & 0 & 0 & 0 \\ -\frac{T}{m} & \frac{N_f}{m} & \frac{T_j}{m} & \frac{N_\alpha + N_f}{mV \cos \alpha_0} \end{bmatrix} \begin{bmatrix} \beta_{TVC} \\ \beta_{fins} \\ \beta_{thr} \\ v_w \end{bmatrix}$$

SS indicators for Dryden step



HF and LF gust responses



Notice that the **Wind-Disturbance-Observer (WDO)** results show a drastic reduction on: **[ss indicators]** the load (°) and drift (m/s) & equivalently **[gust response]** the α (deg) and $z\dot{d}ot$ (m/s)

- **DESCENDO** provides a trade-off between computational efficiency and trajectory optimality which makes it suitable to the extended flight envelope of RLVs
- Earliest application of **robust wind disturbance observation (WDO)** for improved launcher load relief
- Shown that **combined used of TVC/fins** can further improve load relief